



HAL
open science

The Mars Microphone Onboard SuperCam

David Mimoun, Alexandre Cadu, Naomi Murdoch, Baptiste Chide, Anthony Sournac, Yann Parot, Pernelle Bernardi, P. Pilleri, Alexander Stott, Martin Gillier, et al.

► **To cite this version:**

David Mimoun, Alexandre Cadu, Naomi Murdoch, Baptiste Chide, Anthony Sournac, et al.. The Mars Microphone Onboard SuperCam. *Space Science Reviews*, 2023, 219 (1), pp.0. 10.1007/s11214-022-00945-9. hal-03977124

HAL Id: hal-03977124

<https://hal.science/hal-03977124>

Submitted on 17 Mar 2023

HAL is a multi-disciplinary open access archive for the deposit and dissemination of scientific research documents, whether they are published or not. The documents may come from teaching and research institutions in France or abroad, or from public or private research centers.

L'archive ouverte pluridisciplinaire **HAL**, est destinée au dépôt et à la diffusion de documents scientifiques de niveau recherche, publiés ou non, émanant des établissements d'enseignement et de recherche français ou étrangers, des laboratoires publics ou privés.

The Mars Microphone Onboard SuperCam

David Mimoun¹  · Alexandre Cadu¹ · Naomi Murdoch¹ · Baptiste Chide² · Anthony Sournac¹ · Yann Parot² · Pernelle Bernardi³ · P. Pilleri² · Alexander Stott¹ · Martin Gillier¹ · Vishnu Sridhar⁴ · Sylvestre Maurice² · Roger Wiens⁵ · the SuperCam team

Abstract

The “Mars Microphone” is one of the five measurement techniques of SuperCam, an improved version of the ChemCam instrument that has been functioning aboard the Curiosity rover for several years. SuperCam is located on the rover’s Mast Unit, to take advantage of the unique pointing capabilities of the rover’s head. In addition to being the first instrument to record sounds on Mars, the SuperCam Microphone can address several original scientific objectives: the study of sound associated with laser impacts on Martian rocks to better understand their mechanical properties, the improvement of our knowledge of atmospheric phenomena at the surface of Mars such as atmospheric turbulence, convective vortices, dust lifting processes and wind interactions with the rover itself. The microphone also helps our understanding of the sound signature of the different movements of the rover: operations of the robotic arm and the mast, driving on the rough surface of Mars, monitoring of the pumps, etc. The SuperCam Microphone was delivered to the SuperCam team in early 2019 and integrated at the Jet Propulsion Laboratory (JPL), Pasadena, CA with the complete SuperCam instrument. The Mars 2020 Mission launched in July 2020 and landed on Mars on February 18, 2021. The mission operations are expected to last until at least August 2023. The microphone is operating perfectly.

Keywords Mars · Mars 2020 · Perseverance · SuperCam · Microphone · Sound

1 The Mars Microphone

In July 2020, NASA launched a Rover that landed on Mars in February 2021 and has been operating since then on the surface of Mars, in the remnants of the Jezero crater delta which may include ancient sedimentary deposits and water altered materials (Mangold et al. 2021). The Mars 2020 rover, named Perseverance, is dedicated to the study of Mars habitability and the search of potential traces of ancient life, and to the study of the capacity of the

Note by the Editor: This is a Special Communication, linked to the Topical Collection on the Mars 2020 mission published in Space Science Reviews. Space Science Reviews publishes unsolicited Special Communications. These are papers linked to an earlier topical volume/collection, report-type papers, or timely papers dealing with a strong space-science-technology combination (such papers summarize the science and technology of an instrument or mission in one paper).

explored locations environment to sustain life or the potential that the sites visited had to support life (Farley et al. 2020). Like in the previous Mars Science Laboratory (JPL) Curiosity Mars rover, the mission includes a long-duration science laboratory. The Mars 2020 Perseverance rover is capable enough to make in situ, multi-criteria evaluation of samples, and to encapsulate them in sample-return containers left behind for future sample-return missions (Muirhead et al. 2020). Of course, the assessment of present and past habitability includes multidisciplinary measurements; habitability criteria require a thorough evaluation in various thematic fields such as biology, climatology, mineralogy, geology and geochemistry. Among the scientific instruments on board Perseverance, SuperCam (Wiens et al. 2021) provides a rich set of tools to help the Mars 2020 (M2020) Perseverance rover to reach those scientific goals. The SuperCam instrument is an evolution from the successful ChemCam instrument on Mars Science Laboratory (MSL) Curiosity (Maurice et al. 2012). SuperCam is an instrument package capable of four different remote-sensing techniques: Laser-Induced Breakdown Spectroscopy (LIBS), time-resolved fluorescence (TRF), passive visible and infrared reflectance spectroscopy (VISIR) reflectance spectroscopy, and Remote Imagery (RMI). A fifth technique, the sound recording, has been added to complement the LIBS measurements and also to open a new window of measurements on Mars: prior to Mars 2020, no sound had ever been recorded on the surface of Mars. Another microphone has been accommodated on the flanks of the Mars 2020 Perseverance rover, the Entry, Descent and Landing (EDL) microphone. It was designed to record sounds during the descent and shortly after the landing (Maki et al. 2020).

1.1 A Brief History of Planetary Microphones

The SuperCam Microphone is not the first microphone that has been implemented in a space mission, but it has been the first to operate successfully on Mars and to record the first sounds of Mars. The idea of having sounds from Mars, and more generally from other worlds, has an incredible popularity among the general public. The short history of the planetary microphones began with the Grozo 2 instrument during the Venus Venera 13 and 14 missions (Ksanfomaliti et al. 1982).

A successful attempt to record the ‘sound’ of the Huygens probe entry, descent and landing on Titan was made in 2005. The primary focus was to record thunder, but the microphones eventually recorded only aeroacoustic sounds. Even though the acoustic file published was actually a reconstruction from several measurements during the descent through the atmosphere of Titan, it has still been a popular success, downloaded thousands times from the European Space Agency (ESA) website, see e.g. Leighton and White (2004).

The original Mars Microphone instrument, funded by the Planetary Society (Delory et al. 2007) was built for the ill-fated Mars Polar Lander (MPL) mission, which lost contact with Earth shortly after its descent to the Martian surface and was never recovered. However, the worldwide interest in the Mars Microphone project was so intense that immediately following the loss of MPL, an opportunity to fly the microphone experiment was provided by the Centre National d’Etudes Spatiales (CNES), the French Space Agency, on the NetLander mission (Dehant et al. 2004) to Mars in 2007. But NetLander was canceled in 2001, and a Mars microphone was planned to operate on the Phoenix mission (Smith 2004). The microphone included as part of the MARDI (Malin et al. 2009) instrument on Phoenix had originally been developed by the team at Malin Space Science Systems (MSSS) for MARDI on Mars Polar lander but was descope from that mission. The Phoenix MARDI instrument was not operated during EDL due to a potential problem with the spacecraft avionics, not

related to the instrument. One attempt was made to operate it on the surface near the end of the mission, but this was not successful due to commanding errors. No other attempt was made before communications with the spacecraft were lost.

Finally, a last proposal was made by the ISAE-SUPAERO Team to ESA for the (also ill-fated) Schiaparelli descent module. The microphone was planned to be integrated into the Dust Characterisation, Risk Assessment, and Environment analyzer on the Martian Surface (DREAMS) payload package (Esposito et al. 2013) as an add-on to other atmospheric science payloads. The microphone goals were to detect, during the short life of the lander on the Mars ground (up to three days in the most optimistic case), atmospheric related events such as convective vortices, sand saltation noise or any other atmospheric noise. However, some reserves were issued by ESA on the possible science outcome of the instrument and it was finally not implemented.

1.2 SuperCam Instrument Overview

The SuperCam instrument is an evolution from the successful ChemCam instrument on MSL Curiosity (Maurice et al. 2012). In addition to the geologic investigation capabilities, linked to the Laser Induced Breakdown Spectroscopy, or LIBS technique (see Sect. 2.3) it implements a new Raman biological spectroscopic analysis. Another improvement has been made by the addition of color to Remote Micro Imager (RMI), which provides context for the instrument.

The SuperCam package consists of three separate major units: the “Body Unit”, the “Mast Unit” and the “Calibration Targets” (see Fig. 1). The Mast Unit (MU) consists of a telescope with a focusing stage, a pulsed laser and its associated electronics, an infrared spectrometer, a color Complementary metal-oxide-semiconductor (CMOS) micro-imager, and focusing capabilities. A new development for SuperCam is separate optical paths for LIBS (“red line”) and Raman spectroscopy (“green line”), which produces a frequency-doubled beam.

The Body Unit consists of three spectrometers covering the Ultra Violet (UV), violet, and visible and near-infrared ranges needed for LIBS. The UV and violet spectrometers are identical to ChemCam. The visible spectrometer uses a transmission grating and an intensifier so that it can double as the Raman spectrometer. The intensifier allows the rapid time gating needed to remove the background light so that the weak Raman emission signals can be easily observed. A fiber-optic cable, as well as signal and power cable, connects the Mast and Body units.

In addition, a set of calibration targets mounted on the rover will enable periodic calibration of the instrument. A complete description of the instrument can be found in Maurice et al. (2021).

The Mast Unit is provided by Institut de recherche en Astrophysique (IRAP) (funding from CNES), while Los Alamos National Laboratories (LANL) provided the Body Unit. The IRAP and LANL portions are entirely separate mechanically, greatly simplifying the interface controls as well as development across international boundaries. The University of Valladolid (UVa) in Spain is the lead for the SuperCam on-board Calibration Targets.

2 SuperCam Microphone Science Objectives

2.1 Science Objectives Derived from SuperCam

The SuperCam Microphone goal is to record audio signals on the surface of Mars from both natural and artificial origins. Contrarily to previous attempts to operate a microphone on

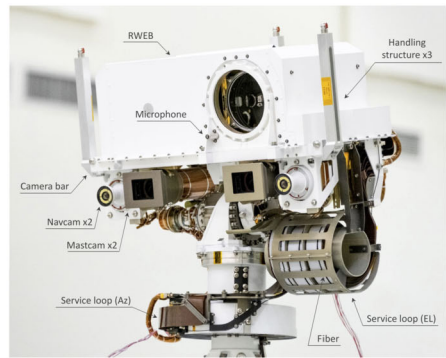
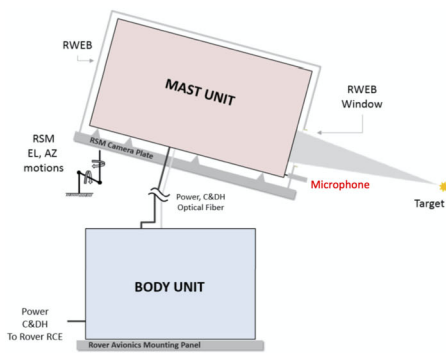


Fig. 1 SuperCam Block diagram (left) - figure modified from Maurice et al. (2021) SuperCam Mast Unit (right) after its integration at JPL - Credits NASA/JPL

Mars, which were primarily for outreach purposes, the primary science objective is to support the SuperCam LIBS investigation. LIBS stands for “Laser Induced Breakdown Spectroscopy” and is the key technique that has been developed in the frame of the ChemCam experiment (Maurice et al. 2012) to analyze – at distance – the composition of the Martian rocks. It uses a powerful laser to ablate rocks and create plasma: the emitted radiation is then be collected by a telescope and its spectrum is analyzed (see e.g. Fig. 6).

The sound recording of the LIBS laser shots provides a unique opportunity to obtain the properties of Martian rocks and soils, mostly related to the rock hardness (Maurice et al. 2021; Chide et al. 2019; Murdoch et al. 2019). This objective is directly linked to the primary science of SuperCam. However, the SuperCam microphone also provides several other scientific opportunities. By providing wind and turbulence measurements, and potentially recording dust devils at a close distance (Chide et al. 2021; Murdoch et al. 2021a,b), the SuperCam Microphone also contributes to the Mars 2020 atmospheric science goals linked to the circulation, weather and climate, the dust cycle and even aeolian processes. From an engineering perspective, the SuperCam microphone enables backup determination of the SuperCam telescope focus (Lanza et al. 2021), and monitoring of artificial sounds emitted by other payloads, e.g. MOXIE (Hecht et al. 2021), or MastCam-Z (Bell et al. 2021), or by the rover operation itself. If we refer to SuperCam Science objectives and goals (Maurice et al. 2021), the SuperCam Microphone complements the experiment for the goals detailed in Fig. 2 and Fig. 3.

It is important to recall that this instrument opens a new window in our Mars observation capabilities, adding for the first time the sense of “hearing” to a rover. The SuperCam Microphone is, therefore, a powerful outreach tool, which draws a lot of general public attention to planetary science.

2.2 Sound Propagation in the Martian Atmosphere

Before the first significant scientific results were achieved, summarized in Maurice et al. (2022), many scientists believed that a Mars microphone would record hardly anything, due to the combination of low pressure of the atmosphere and of the expected attenuation of the sound in a carbon dioxide atmosphere.

Pioneering work had been done notably by Williams (2001) or Bass and Chambers (2001) for the Mars Polar Lander mission: sound propagation on Mars is expected to be

		SuperCam Goals							
		1. Rock identification	2. Sediment stratigraphy	3. Organics & biosignatures	4. Volatiles (H, halogens)	5. Morphology and texture	6. Coatings & Varnishes	7. Regolith charact.	8. Atmosphere charact.
Mission Goals	A. Geologic diversity								
	B1. Habitability								
	B2. Bio-signatures								
	B3. Past life								
	C. Cache samples								
	D2. Dust								
	D3. Weather								

Fig. 2 SuperCam science goals as described in Maurice et al. (2021). The microphone pictures indicate the goals to which the microphone contributes

	Objectives	Comments
SuperCam Goal 1/2/5	Rock Identification, sediment morphology and texture	Characterization of target properties: sound wave amplitude depends on ablated material quantity at a given distance, e.g. (Grad and Mořina 1993)
SuperCam Goal 7	Regolith Characterization	SuperCam microphone will help address soil properties: the acoustic energy of the sound wave depends on material compaction and hardness (Qin and Attenborough 2004; Chide et al. 2019; Murdoch et al. 2019)
SuperCam Goal 8	Atmospheric Characterization	SuperCam microphone secondary goals will help address various atmospheric phenomena such as wind properties, dust devils, turbulence, etc. (Chide et al. 2021; Murdoch et al. 2021a,b)

Fig. 3 Description of the Microphone Goals

similar to within the Earth's stratosphere, with an average atmospheric pressure between 6 and 8 millibars and a mean temperature of about 240 K. These acoustic models predict a frequency-dependent sound speed and attenuation where inflection points at a few kHz result from carbon dioxide molecular relaxation processes (See Fig. 4): in the cold, carbon dioxide Martian atmosphere, a strong attenuation across the audible frequency range is expected. We have based the design of the experiment on this model and considered that the acoustic pressure amplitude follows Equation (1)

$$p(r, f) = p_0 \left(\frac{r_0}{r} \right)^\beta \cdot e^{-\alpha(f) \cdot r} \quad (1)$$

where p is the pressure at a distance r , r_0 the reference distance, p_0 is the pressure at the source, and f the frequency. The β coefficient derives from the geometric attenuation ($\beta = 1$

Fig. 4 Sound attenuation coefficient for an atmosphere of CO₂ at 240K and 740 Pa. Based on the models from Williams (2001) (dashed red line), and Bass and Chambers (2001) (solid red line). A peak in absorption is predicted around 100 Hz by Williams (2001) but this is an error due to a confusion between α and $\alpha\lambda$. Also shown (solid blue line) is the frequency dependent attenuation coefficient for the Earth

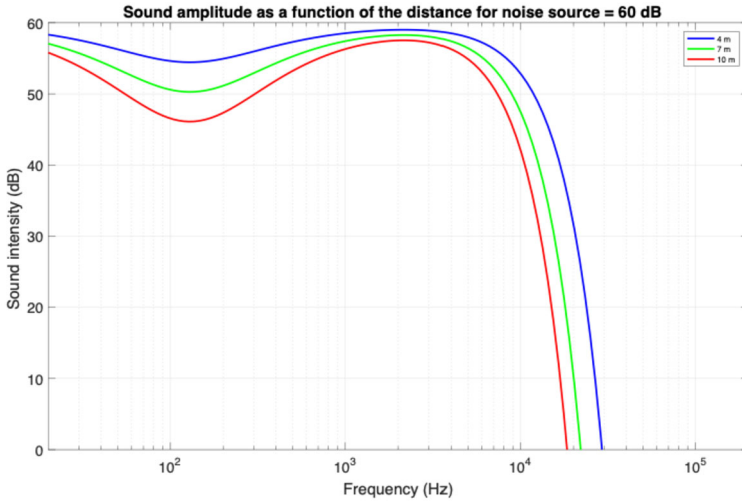
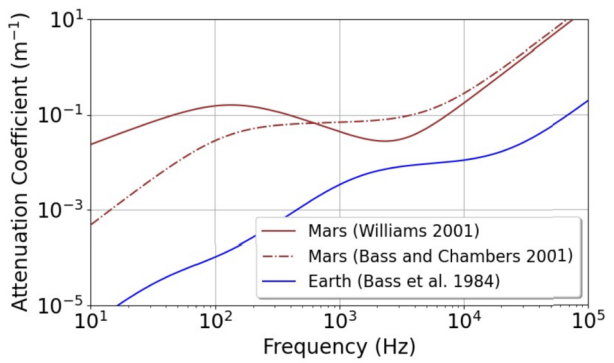


Fig. 5 The sound intensity of a 50 dB source as a function of frequency for three different distances (4 m - blue, 7 m - green and 16 m - red). Derived using the model of Williams (2001)

for a spherical wave and $\beta = 0$ for a plane wave front). $\alpha(f)$ is a frequency-dependent attenuation coefficient that is graphically represented in Fig. 4.

It was predicted that most sounds in the frequency range audible to the human ear (20 Hz–20 kHz) will not propagate over more than some tens of meters, particularly the higher frequency range (see 5). However, the situation improves in the lower frequencies and infrasound region (<20 Hz). Such low acoustic frequencies, produced, for example, by dust devils (e.g. Lorenz and Christie 2015), or bolide impacts (e.g. Williams 2001), could propagate over kilometer ranges. This process has been described e.g. in Martire et al. (2020) in the context of the NASA InSight mission (Banerdt et al. 2020). In order to assess the potential of sound recordings on Mars, and build a science-focused Mars microphone, we have, therefore, chosen to use a double approach: design an instrument based upon these analytical models, and confirm the performance of the instrument with tests in a Martian environment (see Sect. 5).

As it can be derived from Fig. 5, the sound is not expected to propagate significantly at frequencies over 10 kHz, and the maximum distance of recording of a sound of typical

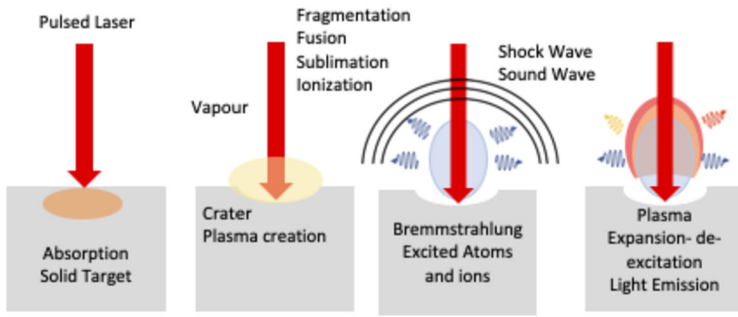


Fig. 6 LIBS: the process of sound emissions - after Rehse (2021)

amplitude (e.g. 60 dB) is relatively limited. To this end, a nominal sampling frequency of 25 kHz is chosen for the SuperCam microphone in order to capture most of the audible signal. An optional 100 kHz frequency has been added to allow the optimization of low-pass filters.

The start of each laser shot is easily detected through their electromagnetic impact on the recording. The difference between the time of this spike and the beginning of the sound arrival can be used to determine the average speed of sound along the targeted direction, providing that the distance between the SuperCam Mast Unit and the target is known. These distances can be known thanks to the 3D model of the environment built on the MastCam-Z stereo view. We were able to measure the variations of the sound speed (Maurice et al. 2022).

2.3 Recording the LIBS Measurements

The first objective of the SuperCam Microphone is to record sounds resulting from the interaction of the laser with the rock targeted by the LIBS technique.

LIBS is a chemical analysis technology that uses a short laser pulse to create a micro-plasma on the surface of the sample. The micro-plasma is then analyzed by a spectrometer, which analyzes the spectrum of the sample to be studied. This technique was invented when the laser first appeared in the 1960s. The term LIBS was introduced in the 1980s in reference to the breakdown of the air by laser pulses during the creation of plasma. This technique, which allows the remote chemical analysis of samples (therefore without contact with potentially dangerous samples, such as radioactive samples), is now experiencing a renewed interest due to the appearance of powerful lasers delivering more powerful pulses. It is also a perfect tool for remote sensing when manipulating samples in a scientific laboratory is challenging or dangerous. The process by which the laser sparks creates a sound is described in Fig. 6.

The interest of this recording is two-fold: first of all, this technique allows remote analysis of the target, without bringing the robotic arm into contact with the mineral to be analyzed. In addition, the first laser impacts vaporize the layer of dust that covers the rock to be analyzed, allowing an analysis of the rock thus uncovered. However in the process the structure of the target is lost. Listening to LIBS sparks provides new information relative to the ablation process that is independent from the LIBS spectrum. From the LIBS literature, the acoustic wave is known to be a product of laser-induced evaporation at high power density of radiation of a sample surface:

$$\Delta P \approx m_{abl} \cdot 1/v_{acw} \cdot 1/r \quad (2)$$

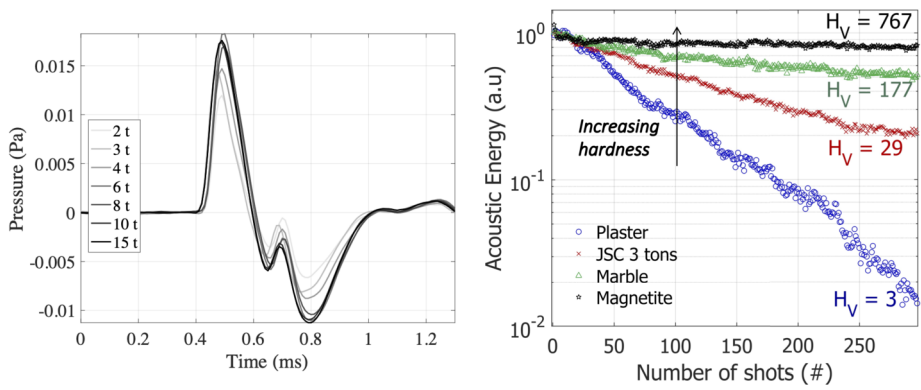


Fig. 7 Relationship between the LIBS acoustic signal and the target. Left: Waveform measured during impacts on samples of Martian soil simulants JSC1 at different levels of compaction - After Murdoch et al. (2019). Right: The rate of decay of acoustic energy during a series of shots depends on the hardness of the target. After Chide et al. (2019)

where v_{acw} and r are the velocity of the acoustic wave front and the distance. Thus, the intensity of the acoustic signal acquired as the peak-to-peak amplitude of acoustic waveform will be proportional to the ablated masses m_{abl} as demonstrated by Chaleard et al. (1997) for aluminum alloys and Grad and Možina (1993) who used various ceramics. In our experiments with the SuperCam microphone (Murdoch et al. 2019), we used soil simulant targets, to demonstrate that the acoustic signal associated with the plasma formation during the LIBS experiment varied as a function of the target compaction. Then Chide et al. (2019) compared in detail the shot-to-shot evolution of acoustic energy with the laser-induced crater morphology and plasma emission lines. The chosen targets are a set of geological targets of various origins and hardness; the depth and volume of the craters created by the LIBS impacts have been profiled and analyzed with the associated sound recording. The observable here is the acoustic energy recorded by the microphone. A good proxy of this acoustic energy is the integral of the waveform. The decrease of the acoustic energy as a function of the number of shots is well correlated with the target hardness/density (Fig. 7). This can be explained as the acoustic energy source originates in the hole created by the sparks: shape and volume of the hole vary as a function of the number of shots, changing the source geometric properties.

Therefore, listening to laser-induced sparks can complement the LIBS experiment by providing constraints on the hardness/density of the targeted rock. An interesting consequence of the sensitivity of the acoustic signal to target hardness/density is that we can interpret a rupture of the shot-to-shot energy change as a proxy for the existence of a rock coating at the surface of the target, as described in Lanza et al. (2020).

2.4 Atmospheric Science

The key atmospheric science goal of the microphone is to characterize the Martian atmospheric dynamics at high frequency – much higher than Perseverance’s Mars Environmental Dynamics Analyzer (MEDA) instrument suite, which makes measurement at up to 2 sample per second (sps) for the wind, and 1 sps for the pressure (Rodriguez-Manfredi et al. 2021). The microphone measures high frequency variations in the dynamic pressure, and such pressure fluctuations are crucial to understanding the Martian climate, including the diurnal and seasonal evolution. Therefore, the atmospheric science investigations of the microphone,

can be linked to the Mars 2020 mission high-level atmospheric investigations and science goals:

- What controls the circulation, weather and climate?
- What controls the dust cycle?
- Aeolian processes and rates

2.4.1 Measurement of the Atmospheric Turbulence

Atmospheric turbulence is a key property of the Martian atmosphere. The thinness of its atmosphere associated to the thermal properties of its sandy surface pave the way for strong instabilities of the boundary layer gradient, resulting in convective turbulence (e.g. Tillman et al. 1994). Pressure fluctuations and wind gusts (both observable on the microphone) are manifestations of convective motions in the atmosphere. These convective motions are linked to dust motion and lifting, and there is also a link between the observed pressure fluctuations and the atmospheric opacity measurements (e.g., Ullán et al. 2017).

The turbulent properties of the Planetary Boundary layer (PBL) are key to understanding the conditions of the Martian atmosphere (see Spiga et al. 2018; Chatain et al. 2021; Temel et al. 2022). Following our work on the Mars atmospheric turbulence spectrum (Mimoun et al. 2017; Temel et al. 2022) based on wind, pressure and infrasound measurements, we use the SuperCam microphone to extend the measurements of the InSight and Perseverance meteorological suites to higher frequencies. The microphone allows us to characterize the Martian dynamic pressure fluctuations at high frequency for the first time, giving us information about the spectral content of high frequency turbulence.

In addition, the combination of MEDA and microphone data allow us to investigate the full energy spectrum of the atmosphere, and its potential variations at hourly, daily and seasonal scales (Chatain et al. 2021). In addition, we are able to identify the transition frequency (or frequencies) between the various regimes of the Martian atmosphere at the Jezero site, see Maurice et al. (2022).

2.4.2 Measurement of the Wind Speed

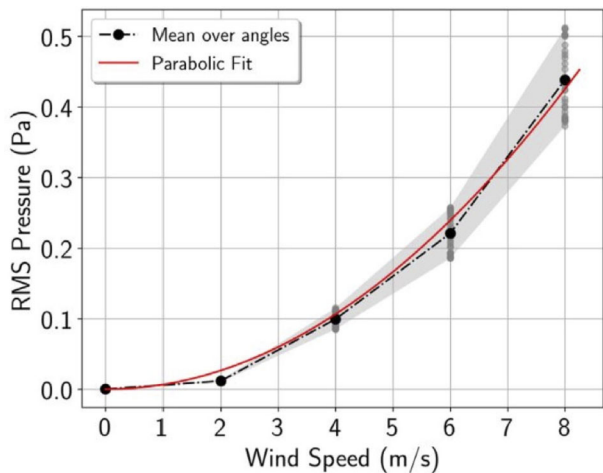
A first attempt to measure the wind speed thanks to an interplanetary microphone has been done on Venus (Ksanfomaliti et al. 1983). This measurement is based on the following relationship (as described in Morgan and Raspert 1992.)

$$P = \rho UV \quad (3)$$

where P is the sound pressure, ρ the atmospheric density, U the variation of wind speed and V the mean wind speed. Lorenz et al. (2017) used data collected from the Aarhus Martian wind tunnel to demonstrate the potential for using a microphone as a wind speed sensor on Mars. Specifically, they report that the Root Mean Square (RMS) voltage measured by the microphone varies with the wind speed. During the end-to-end tests of the SuperCam Microphone in the same wind tunnel (see Sect. 5 and Murdoch et al. 2019; Chide et al. 2021), we were also able to correlate the wind speed to the SuperCam microphone measurements (Fig. 8), and quantify the influence of the SuperCam Mast Unit orientation with respect to the wind direction.

As the wind tunnel is not fully representative of the environment on Mars, an in-situ calibration is required after the landing, with microphone measurements being taken from 360° around the mast unit, while simultaneously measuring the wind speed and direction

Fig. 8 Relationship between wind Speed and RMS sound pressure level measured by the microphone during Aarhus tests - After Chide et al. (2021). RMS is calculated over the 100-500 Hz band. Gray dots are values for different angles of the Mast Unit with reference to the wind



along with temperature and pressure using MEDA. This in-situ calibration aims to uncouple the effect of several parameters, such as the Mast Unit orientation, pressure, ground and air temperature to understand the wind field. Preliminary analyses indicate that machine learning methods could be used to optimize the measurement.

2.4.3 Acoustic Detection of Dust Devils and Convective Vortices

Dust devils are convective vortices, usually of a few meters to tens of meters in diameter, that lift and transport dust particles. This phenomenon has been witnessed on Earth since centuries in arid regions, or more generally in regions where the convective activity of the atmosphere is important (Balme and Greeley 2006). Vortices and dust devils are also common on Mars see e.g. Ferri et al. (2003), Murphy et al. (2016), Perrin et al. (2020).

As described in Lorenz and Christie (2015), convective vortices have a low frequency sonic counterpart that has already been detected on Earth. The microphone can record the sound pressure level associated with dust devil encounters. However, Murdoch et al. (2021a) explain that the sizing vortex signal on the SuperCam Microphone will likely be the pressure fluctuations induced by the wind dynamic pressure (Fig. 9, left). Such a signal has also been observed with microphones in terrestrial field experiments (Lorenz et al. 2017).

In any case, in order to measure the vortex winds, or to record any possible infrasound generated by vortices despite the sound attenuation of the Martian atmosphere, a very close-range vortex encounter is necessary as described in Murdoch et al. (2021a).

2.5 Monitoring Sounds from the Rover

The primary objectives of the SuperCam microphone are related to Mars 2020 science. However, these objectives can be completed by several opportunistic secondary objectives that can be classified in roughly two types of objectives: first, “engineering support”, with the recording of the various sounds produced by the Mars Perseverance rover. As during our everyday life, listening to the noise from mechanical devices provides a quick diagnosis on the inner workings of a complex piece of engineering. The SuperCam microphone team collaborates with various other instrument teams (e.g. MOXIE pumps Hecht et al. 2021), or MastCam to help them to record a “reference” noise recording that will serve to help

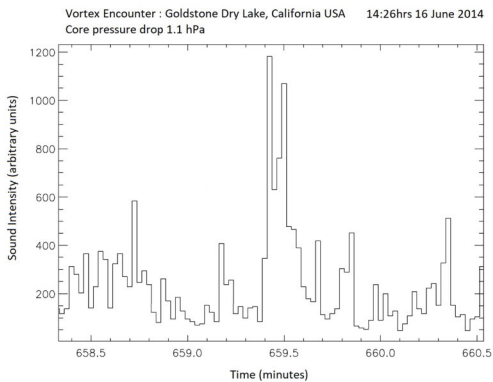
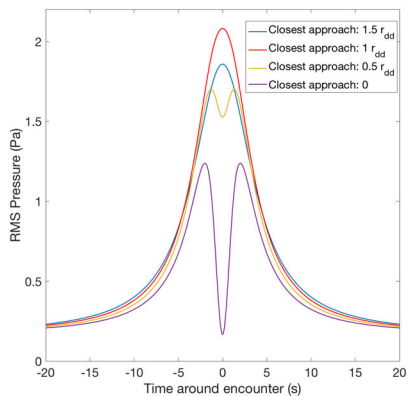


Fig. 9 Left: Simulated SuperCam Microphone vortex signals as a function of the closest approach distance. Vortex parameters: 10 m radius, 5 Pa core pressure drop, advecting past the microphone at 5 m/s (Murdoch et al. 2021a). Right: Acoustic recording of a dust devil vortex (Murdoch et al. 2021a)

Table 1 Possible sound/acoustic sources, with initial likelihood of success

Potential Sound Source	Interest	Planning	Achieved?	Comment
MOXIE	Pump behavior	Yes	Yes	Planned before launch
MastCam-Z	Motors Monitoring	Yes	Yes	
Helicopter	Heli sound and video	Yes	Yes	See section TBD
Drill	Drill surveillance	No	No	Not tested
Rover Wheels	Soil interaction	No	No	Recorded by EDL microphone

investigate any later issue in the instrument operation. The Table 1 makes a summary of possible sound recordings, and the Fig. 36 summarizes all recordings done up to sol 450.

Also, there has been a sustained interest in just listening to sounds from Mars, in order to engage the public in planetary science. Wind blowing on another planet, rover sounds recordings, and even the Mars 2020 helicopter recordings are of great interest for public outreach.

2.6 Requirements Summary

2.6.1 Science Related Requirements

Due to its strong coupling with SuperCam LIBS investigation on rock hardness, the microphone was designed to be able to record the pressure wave generated by the LIBS shot, which has typical maximum amplitude of 5 Pa, at a distance of 4 meters from the rover mast, in a Martian atmosphere (see Fig. 10). In order to support the SuperCam geological investigation with classical signal processing methods, the signal-to-noise ratio (SNR) of the recording must be greater than 10 dB.

The expected bandwidth, as described in Sect. 2.3 ranges from 20 Hz to 10 kHz. The optimal sampling frequency is 100 kHz to satisfy anti-aliasing criteria. A degraded mode

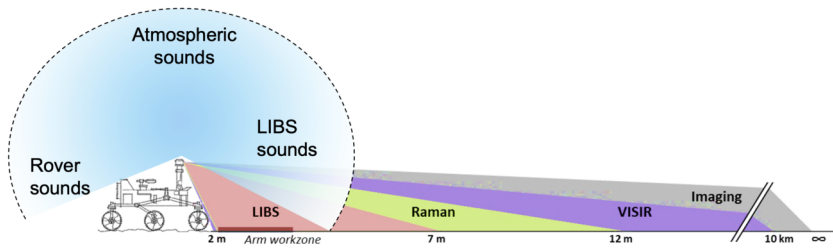


Fig. 10 Microphone range among the various SuperCam techniques. All techniques can operate at close range

allows a 25 kHz sampling frequency in order to save telemetry and increase the recording duration. The amplification gain must be tunable to be able to cope with various signal-to-noise ratios. This variability in the signal-to-noise ratio comes from the potentially small amplitude of the acoustic signals, possibly linked the variation in distance of the various targets (the requirement is to measure up to 4 meters), and to the variability in the LIBS acoustic counterpart depending on the target material properties, and on the background noise (wind). We have chosen to keep the analog/digital (A/D) conversion dynamic higher than 60 dB to ensure the quantization effects are negligible with respect to the other error contributors.

As the Martian thermal environment is harsh, the microphone also includes a temperature sensor with relative accuracy of 1 K in order to compensate potential deviations in transfer function and noise. Test results (see Sect. 5) have, however, demonstrated that the sensitivity to temperature is negligible with respect to the calibration capabilities, for both the microphone and its proximity electronics.

The microphone design must also comply with the Martian wind as a potential source of perturbation with respect to the other signals of interest. The acquired signal must not be saturated by the effects of wind up to 1σ of the speed distribution as stated in the Mars 2020 Environment Requirements Document, which is 6 m/s. The test results (see Sect. 5) have shown that the saturation of the electronics occurs beyond a wind speed of 8 m/s and that the frequency content is limited to the lowest frequencies (below 1 kHz), whereas the LIBS signal is mainly above 2 kHz. Usual filtering methods can then be used to separate those signals, provided that saturation is avoided (Murdoch et al. 2019).

2.6.2 Functional and Design Requirements

The microphone was integrated late in the development of the SuperCam Mast Unit. It was agreed with the Mars 2020 project that the microphone would have been descope'd at any time if it had become a threat to other investigations. Fortunately, it survived the many challenges inherent to a space project. This specificity led to a strong design constraint: instead of having its own acquisition, the microphone “piggy backed” on existing the acquisition system of the SuperCam instrument, and uses the same A/D channel as the laser house-keeping. This led to minor operational constraints: the SuperCam team is not able to use the laser temperature housekeeping together with the microphone acquisition, and the total volume of an acquisition (and therefore its duration) is limited.

The total amount of data for one acquisition cannot exceed 8 MB, which is the memory size allocated to one RMI (Remote Micro-Imager) image. This leads to a maximum time of recording of 41 or 167 seconds depending on the chosen sampling frequency. As part of

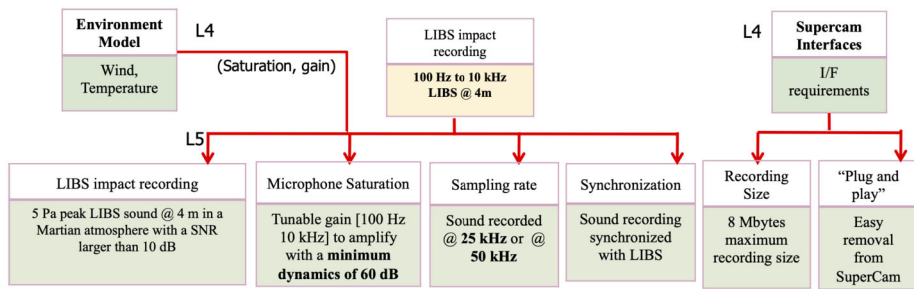


Fig. 11 SuperCam Microphone requirements flowdown. L4 and L5 are requirement levels 4 and 5, respectively

the telemetry reduction effort, a filtering and decimation algorithm has been included in the SuperCam Body Unit (BU) flight software. The decimation factor is fixed to 4, while the 65-coefficient FIR filter ensures a rejection greater than 60 dB beyond 10 kHz.

The synchronization of the microphone recordings with the LIBS shots is mandatory, and is managed at higher level in the SuperCam Mast Unit. Thus, the amount of data necessary for the LIBS analysis can be reduced down to the minimum time window required to match the sound propagation delay and the LIBS signal duration constraints. In order to reduce the data volume, a specific “pulsed” mode has been introduced, in order to be able to record only the LIBS waveforms (as a consequence, this mode cannot be used to study wind turbulence).

The microphone is mounted beside the SuperCam telescope input window holder, in order to face in the direction of the laser target, and detect the acoustic wave without any obstacles. The microphone is, however, omnidirectional for the lowest frequencies, even though it is limited by the surrounding large scale elements (Remote Warm Electronics Box (RWEB), Mast Unit, Rover body, etc.) once integrated to the rest of the system.

The microphone, directly exposed to the Martian environment undergoes daily temperature variations from $-80\text{ }^{\circ}\text{C}$ to $0\text{ }^{\circ}\text{C}$ and is qualified over a range from $-135\text{ }^{\circ}\text{C}$ to $+60\text{ }^{\circ}\text{C}$. The electronics, unable to operate properly at such low temperature, are attached to the Optics Box (OBOX) (SuperCam Subsystem) in order to be protected inside the Remote Warm Electronics Box surrounding the SuperCam instrument (RWEB), and they are qualified over a temperature range from $-55\text{ }^{\circ}\text{C}$ to $+60\text{ }^{\circ}\text{C}$.

2.6.3 Requirements Flowdown

The summary of science and design requirements has allowed us to setup the requirements flow-down for the microphone (Fig. 11). The requirements for the SuperCam Microphone also included small mass and size, a rugged, robust design, and resistance to extreme conditions, including radiation exposure and low temperatures.

3 Instrument Design

3.1 Functional Description

The microphone is composed of two main parts: the microphone sensor located outside of the RWEB (see Fig. 10), and the Front End Electronics (FEE) located inside the RWEB. The functional architecture is described Fig. 10 for the functional. The purpose of the FEE

Fig. 12 Microphone subsystems overview. (Left) The Front-end electronics (FEE) box. (Right) The FEE and the SuperCam Microphone cylinder or “finger”

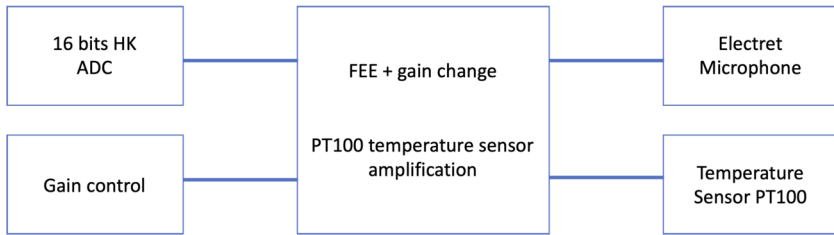
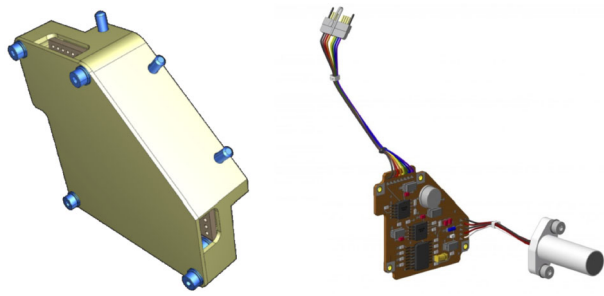


Fig. 13 Microphone functional overview

is to amplify the microphone output for acquisition by the housekeeping Analog to Digital Converter (ADC) of the Instrument Digital Processing Unit (DPU). Figure 12 describes the various parts of the SuperCam Microphone.

The microphone sensor is exposed to the external environment, and is embedded in a cylinder required to pass through the RWEB. The microphone and the PT100 used for the temperature housekeeping are sealed in glue potting to avoid any unwanted motion.

Figure 13 depicts the functional overview of the microphone subsystem. The sound wave (pressure fluctuation) is converted into a voltage by the microphone finger (see Fig. 17) outside the RWEB (Remote Warm Electronic Box). The resulting voltage is amplified by the Front End Electronics (FEE) located inside the RWEB. The FEE integrates a selectable gain (4 values) to match as closely as possible the input voltage range of Laser housekeeping ADC, under any kind of signal amplitude. The recording is stored in the DPU memory, before being downloaded by the Body Unit software, and then stored in a non-volatile memory until the ground data download operations.

The electret microphone component (Fig. 14) is a Component Off the Shelf (COTS) component. It is the same commercial microphone sensor as used on the Mars Polar Lander and the Phoenix missions (Delory et al. 2007; Smith 2004). It sits outside the RWEB, at the tip of a 3 cm sandblasted aluminum “finger” (Fig. 39). Hence the echo from the RWEB itself arrives between 222 μ s and 277 μ s after the direct signal (on Mars). A temperature sensor is also potted inside the microphone stand.

The temperature sensor, a PT100 thermo-resistor, is powered by the same FEE, and the resulting voltage is amplified to provide a sufficiently large signal to the 16-bits ADC of the DPU, dedicated to the precise housekeeping data acquisition of the SuperCam Mast Unit. The microphone temperature data is stored together with the other SuperCam MU housekeeping data.

A shielded cable connects the microphone and temperature sensors to the FEE inside the OBOX (Fig. 14). The harness consists of five Manganin wires to limit the thermal leak.

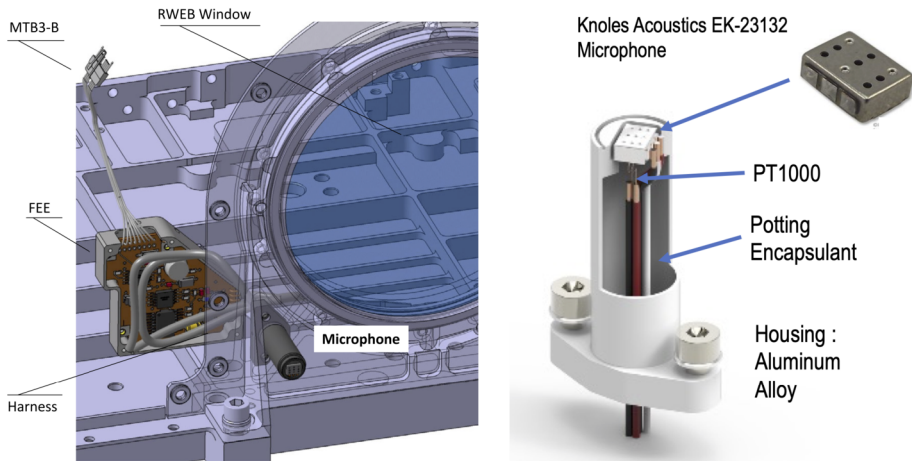


Fig. 14 (Left) Microphone finger implementation overview. (Right) Microphone assembly description. It encloses the microphone sensor, and a PT 1000 temperature sensor into an aluminum casing. The whole interior is filled with a cold-resistant E505 potting

When the electret microphone is at $-120\text{ }^{\circ}\text{C}$ and the OBOX at $-35\text{ }^{\circ}\text{C}$, the power drawn from the survival heaters by the microphone is only 30 mW, four times smaller than for standard copper wires of the same diameter.

The role of the FEE is to amplify and filter the analogic signal and to collect temperature data. A first stage amplifies the signal by a factor $\times 15$, a second stage by a controllable gain, $\times 2$, $\times 4$, $\times 16$, and $\times 64$. The digitalization of the signal is performed by a fast 12-bit ADC on the instrument DPU board. To avoid failure propagation, two short-circuit protections are implemented for the microphone and the operational amplifiers.

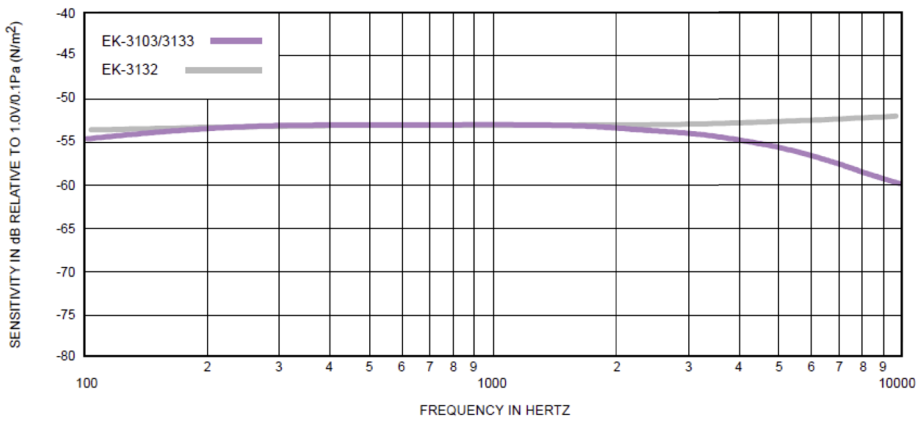
We had initially considered to implement a grid to protect the microphone sensor from Martian dust, but the decrease in sensitivity of the overall assembly when the grid was present led us to favor the instrument performance and remove the grid from the design.

3.1.1 Microphone Component Properties

The SuperCam microphone is a Knowles EK-23132 microphone (Fig. 14). This is an electret based sensor, using a charged membrane, whose movement due to pressure fluctuations alters the capacitance of the sensor, which is then read as a signal. The EK-23132, originally selected for the NASA Mars Polar Lander (MPL) (Delory et al. 2007), is the lowest noise microphone manufactured by Knowles, and in our experience has a sensitivity superior to similar microphones made by other manufacturers. It is designed to be inherently rugged, capable of withstanding severe environmental conditions, and has a low vibration and shock sensitivity. The microphone contains a Bipolar Junction Transistor (BJT) that amplifies the charge variations caused by the membrane motion, transforming this signal into a voltage level through an output bypass resistor.

EK-23132 sensitivity is 29.6 mV/Pa at 1 kHz without any stage of amplification. Its dimensions are 5.6 mm \times 3 mm.

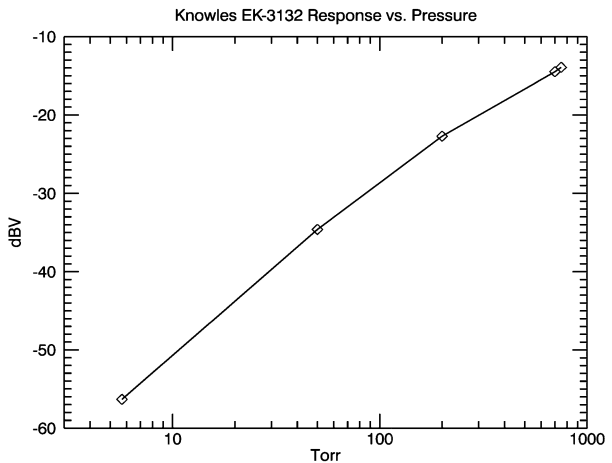
Figure 15 shows the EK-23132 sensitivity and frequency response. Theoretically, the sensitivity of the microphone scales as the acoustic impedance ρc , where ρ is the density



Open circuit sensitivity with 1.3VDC supply

Fig. 15 Microphone sensitivity. The EK-3132 underwent a full qualification process, and was tested for its performance at low atmospheric pressures, low temperatures, and for radiation resistance. Low-pressure tests over a variety of temperatures were conducted in air using standard thermal vacuum chambers. Figure from EK3132 data sheet

Fig. 16 Output in dBV (decibels relative to 1V output) for the EK-23132 as a function of atmospheric pressure in Torr - from EK3132 data sheet



of the gas and c the sound speed. ρ_c for Mars is $\sim 0.01\rho_c$ for Earth Sparrow (1999), thus reducing ρ by 100 for constant c in air achieves a similar effect.

3.1.2 Proximity Electronics

The microphone front-end electronics (FEE) has four functions

1. Amplification of the microphone signal
2. Gain switch (2, 8, 32 and 64)
3. PT100 temperature resistance to voltage conversion
4. Microphone power supply +3.3 V
5. Interface with the O-BOX

Table 2 Gains of the microphone electronics and conversion to physical units. This table includes all amplification gains - fixed and tunable

Gain Number	Measured FEE Gain [V/V]	Total Sensitivity [V/Pa]	Total Sensitivity [LSB/Pa]
Gain 0	29	0.6	491
Gain 1	57	1.2	983
Gain 2	240	5.2	4262
Gain 3	972	21.0	17213

Fig. 17 Microphone hardware during integration



The FEE ensures the polarization of the components and the amplification of the microphone signal. Amplification is done with two stages. The first amplification is fixed, the second amplifier has a selectable gain of 2, 4, 16 or 64 and a bandwidth from 20 Hz to 10 kHz. High gains (32 and 64) have been designed to optimize the SNR with respect to the LIBS sound recordings made in lab. Low gains (2 and 4) are meant to record environmental noise while avoiding saturation due to e.g., wind gusts.

The FEE is directly controlled by the SuperCam power unit (DPU). The measured total gain and the total sensitivity of the microphone flight model at 1 kHz and its electronics are presented in the Table 2. These are the beginning-of-life values but, as mentioned above, we do expect some evolution in the microphone sensitivity over time. The FEE also provides the output of the PT100 temperature probe. The total sensitivity of the temperature measurement is 3.96 mV/K. The output voltage is shifted by a nominal offset of 1.029 V at 0 °C.

The whole design has been made keeping in mind the protection of the SuperCam main electronics. Therefore, a protection against failure, shorts, saturation or single event transient (SET) has been implemented at the input of the FEE. The total power consumption of the microphone FEE is about 20 mW, on $+/- 5$ V. Figure 12 shows the flight model of the FEE during its final inspection before delivery. The FEE box mechanical design is very straightforward: a simple 0.5 mm aluminum box enclosing the FEE (Fig. 12, left). The FEE box is connected to the chassis mass.

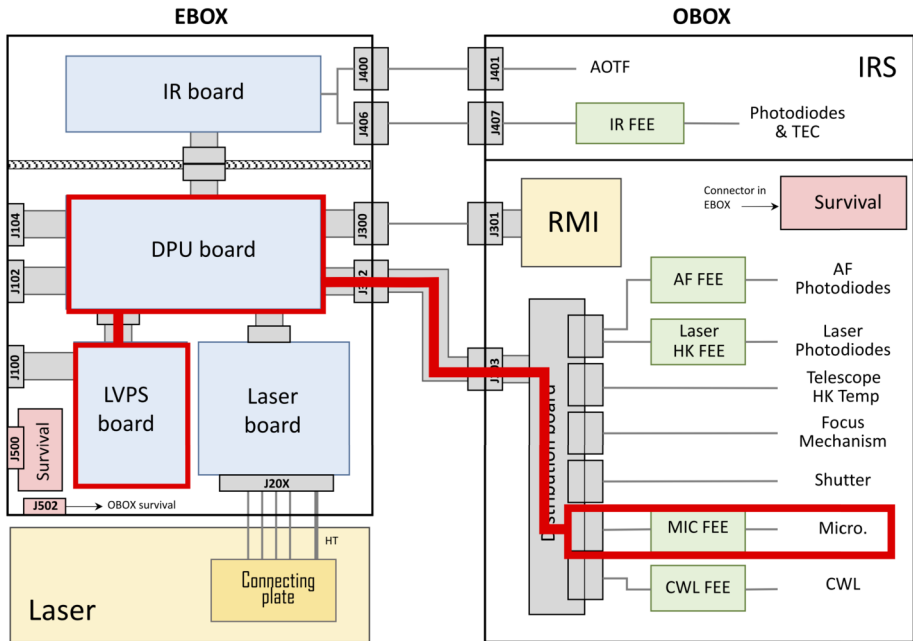


Fig. 18 Microphone Data Handling Architecture. The Microphone data processing takes mainly place in the SuperCam Mast Unit. Figure modified after Maurice et al. (2021)

3.1.3 Microphone Assembly Thermal Design

The temperature range of the FEE is standard: the parts and process selected allow the design to cope with the required temperature range. However, the MIC temperature range is extended down to $-130\text{ }^{\circ}\text{C}$ (lowest possible temperature on Mars), therefore a dedicated qualification has been done for the microphone assembly. Due to the external location of the microphone, the thermal architecture has to minimize the microphone thermal leaks. If a standard strategy using cables and shielding was applied, the conductance of the cable between the microphone assembly and its FEE would be too high to cope with the instrument safe mode heating power requirements. We have, therefore, chosen to implement a thermal leak reduction for the cable, thanks to “athermous” ManganinTM wires, an alloy that conducts current but has a low thermal conductivity.

3.1.4 Data Handling

As required by the instrument design, the SuperCam Microphone is mostly managed by the SuperCam Mast Unit. An overview of data handling architecture is depicted in Fig. 18. The SuperCam Body Unit (BU) is mostly in charge of implementing the data storage, as well as the interface with the Rover. The Mast Unit controls various subsystems, such as the laser, autofocus, microphone, infrared spectrometer (IRS), RMI, and synchronous dynamic random access memory (SDRAM).

The Microphone driver derives from the laser HouseKeeping driver which drives the high-speed ADC (sampling frequency up to 100 kHz) and stores data. This driver is also called by the laser driver to synchronize the recording to the LIBS shots when needed. The

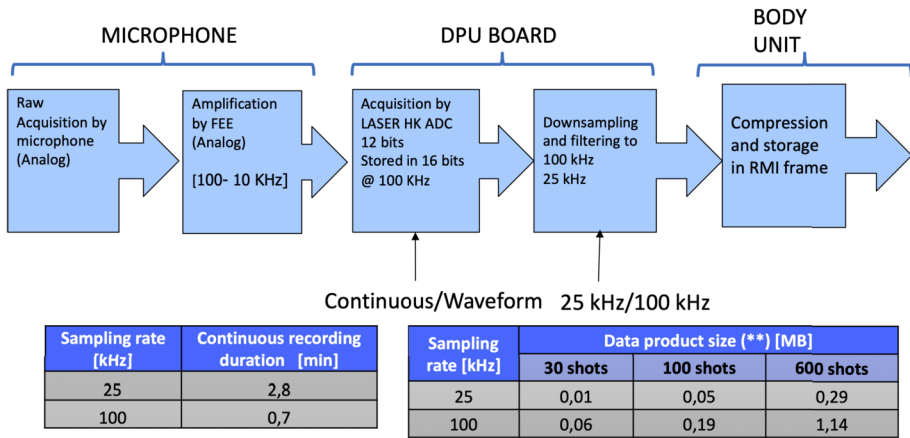


Fig. 19 Microphone data processing. A schematic overview of the data processing. The sampling rate and duration depend on the operational mode of the microphone (see Sect. 3.1.5)

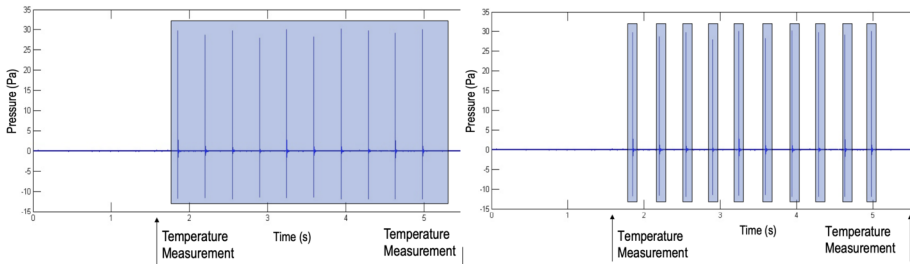


Fig. 20 Graphical representation of MIC standalone / MIC + LIBS continuous mode / MIC + LIBS pulsed mode

DPU Unit controls the microphone. Due to the SuperCam Body Unit software limitations, the recording is limited to a 8 MB data product size. An overview of the processing is shown in Fig. 19.

3.1.5 Operation Modes

The Microphone has three modes of operation (see also Fig. 20):

1. **MIC standalone:** this mode is mostly dedicated to the study of natural (winds) or artificial (rover, helicopter, ...) sounds. It can also be used in coordination with other payloads such as the MastCam-Z or MOXIE. We also call it sometimes “Passive mode”.
2. **MIC + LIBS continuous mode:** used to record sound continuously during a LIBS burst.
3. **MIC + LIBS Pulsed mode:** used to sample specifically the LIBS burst. The sound recording starts less than 1 ms before the laser pulsed is emitted and runs during 60 ms for each shot (except the last one kept for laser data). It allows to keep data only related to the study of the LIBS shots. The timing for the pulsed mode is shown in Fig. 21.

For these 3 modes, we can use the four possible gains (from 0 to 3). Due to storage capability, the recording duration is, at most, 167 s for a sampling frequency of 25 kHz, and 41 s for

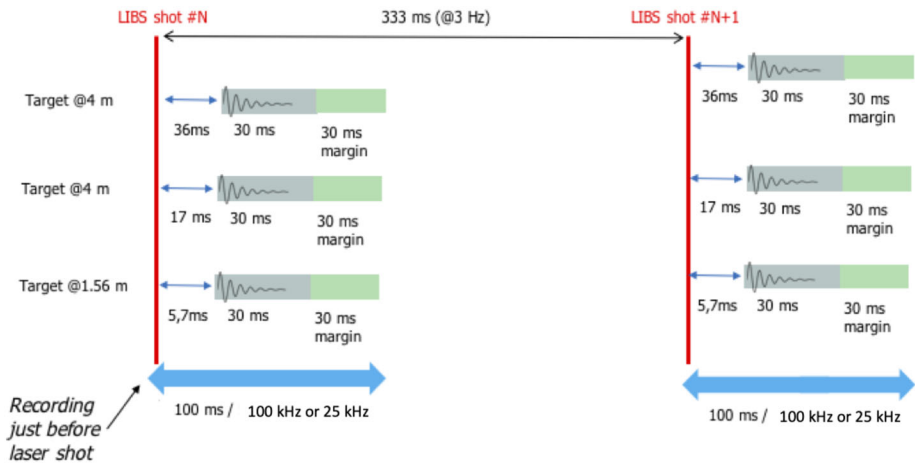


Fig. 21 Microphone pulsed mode timing. The cycle is based on the SuperCam laser raster of 333 ms. The pulsed mode will record 100 ms every 333 ms. This will allow the timing to accommodate all possible distances of the SuperCam LIBS target

a sampling frequency of 100 kHz. An optional decimation algorithm is also implemented in the Body Unit to down sample the data from 100 kHz to 25 kHz. The gain settings depend mostly on environmental noise and LIBS target distance.

4 Performance Model

4.1 Microphone Model

The frequency response of the microphone is established with respect to the manufacturer data-sheet. However, to perform an extended analysis of the instrument, it is necessary to consider a larger frequency band (at least from 10 Hz up to 100 kHz). The microphone was then modeled with a first order high-pass filter ($f_{HP,M} = 30$ Hz) and a second-order low-pass filter ($f_{LP,M} = 15$ kHz, $h_M = 0.2$), and adjusted in amplitude (Microphone sensitivity = 22.4 mV/Pa). The resulting transfer function is described by Equation (4)

$$H_n(f) = S_M \frac{j \left(\frac{f}{f_{HP,M}} \right)}{1 + j \left(\frac{f}{f_{HP,M}} \right)} \frac{1}{1 + 2j H_m \left(\frac{f}{f_{LP,M}} \right) - \left(\frac{f}{f_{LP,M}} \right)^2} \quad (4)$$

and compared to data sheet values. The model is justified at low and high frequencies by the typical sensitivity of similar products of Knowles Electronics. However, without the real damping factor and the cutoff frequency, only likely assumptions have been made so far. The resonance above 10 kHz might have a more complex description than a second-order response, due to the microphone inlet. This is particularly important for the phase modeling and filtering considerations.

4.2 FEE Transfer Function Models

The microphone electronics transfer function (Fig. 22) is the response of two 1st order band-pass filters, plus the output stage representing the behavior of the level shifter (+2.5 V ref-

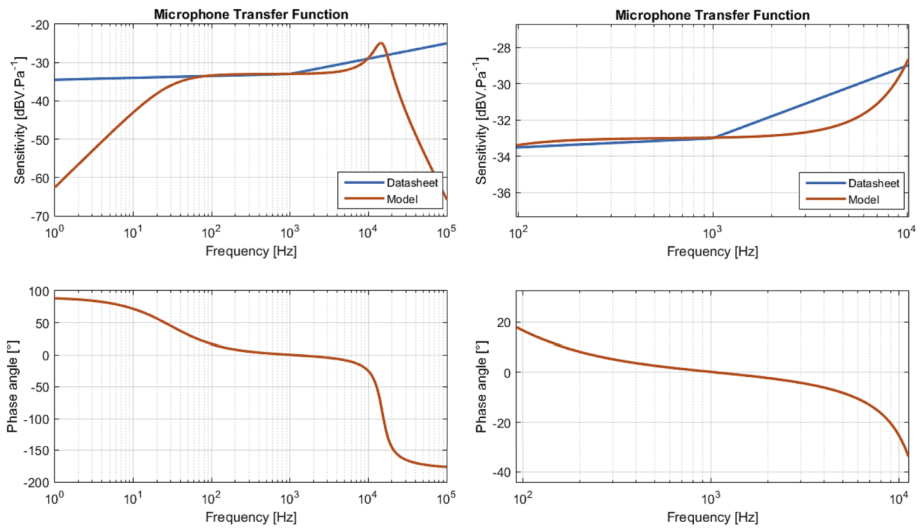


Fig. 22 Theoretical Transfer functions of the microphone model compared to the data sheet. Left: Full bandwidth. Right: Zoom on the band 20 Hz – 10 kHz

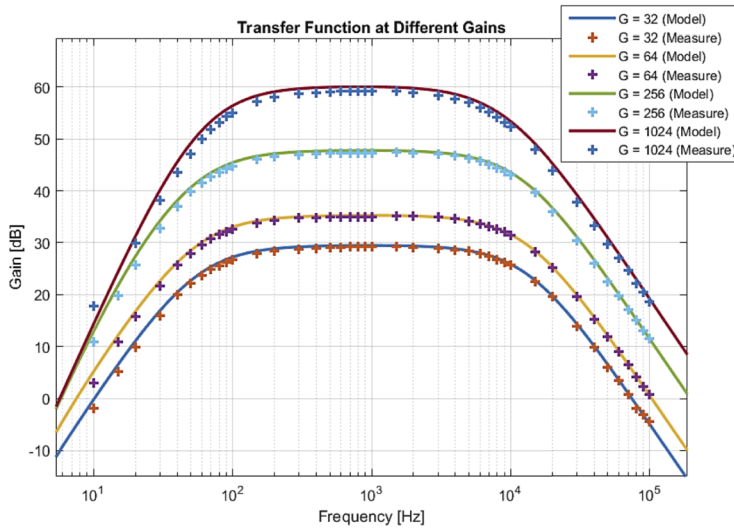
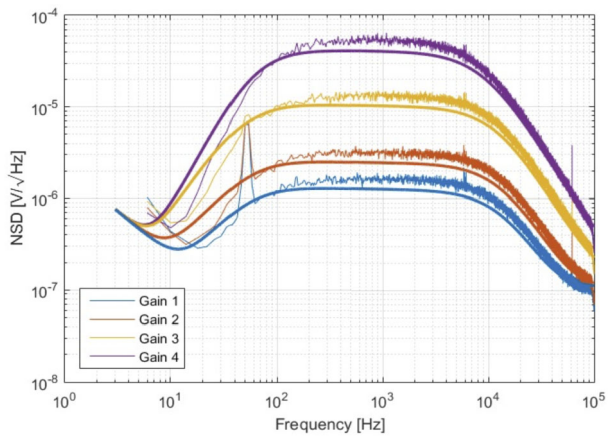


Fig. 23 Comparison of the models (solid lines) with the measurements (+ symbols) of the amplification electronics transfer function (amplitude only)

erence and associated passive components) and a high impedance input (buffer or oscilloscope). It is modeled by including the effect of the non-perfect operational amplifiers. The comparisons of the theoretical results with the measurements are presented Fig. 23. The model is able to reproduce the transfer function amplitude with a precision inferior to 1 dB.

Fig. 24 Comparison between the front-end electronics noise (amplitude) spectral density models (plain lines) and the measurements (noisy curves) for all gains at +25 °C. Note that the remaining 50 Hz peak is due to the difficulty obtaining a clean EMC environment in the lab



4.3 Overall System Noise

The electronic noise is measured with an oscilloscope as the root mean square value of the signal when no input signal is applied to the circuit. Theoretical values computed with the model and measurements are presented in Fig. 24. The order of magnitude of the noise is well reproduced by the model. The remaining small discrepancies are due to the simplifications made in our model. For comparison, an ADC Least Significant Bit (LSB) with an input voltage range of 5 V and 12 bits of resolution is about 1.2 mV. Therefore, the lowest gains (Gains 0 and 1, see Table 2) can be used to improve the maximum input range without saturating the ADC, whereas the highest gains (Gains 2 and 3, see Table 2) are more relevant for the recordings of low amplitude signals and the characterization of background noises.

4.4 Theoretical SNR for LIBS

The complete transfer function amplitudes (sensitivities), including the microphone plus the front-end electronics, are presented in Fig. 25. Each curve corresponds to a defined gain of the second stage of amplification. The LIBS signal amplitude shape used has been derived from recordings made in the lab with calibrated microphones.

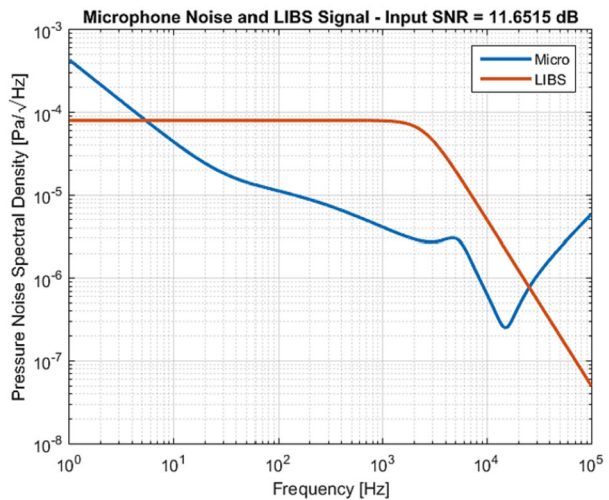
5 Microphone Verification Process

5.1 Microphone Part Verification

Given that the microphone is a COTS component, its integration into a space instrument development required some additional qualifications. A batch of a hundred components was procured from the same manufacturer sub-lot, in order to perform all the necessary tests and integration processes. The whole process is summarized in Fig. 26.

First, an entrance visual inspection was performed to verify the lot and sub-lot numbers of each part. Second, a serial number marking operation was performed to provide a non-ambiguous traceability of each part. Then an initial performance test was performed to track potential degradation during further operations by comparison. The test was based on noise,

Fig. 25 Comparison between the equivalent input noise and the LIBS signal



bias, and sensitivity measurements in a contained acoustic bench, which is dedicated to the whole process. The main group of components (71 parts) underwent vibration, pin tests and re-tinning operation, whereas two other groups were dedicated respectively to radiation and Destructive Physical Analysis (DPA). After the main group performance verification, five parts were finally extracted for internal X-ray inspection and surface electron spectroscopy of the solder pads. No physical or performance degradation was observed at this step. The 20 best components in terms of acoustic sensitivity were then selected to be integrated in the microphone assembly. Six were allocated to package qualification and verification (PQV) (package qualification and verification) testing and further inspections, the five best assemblies were used for the final qualification thermal test of the models eligible for flight. Contrary to the rest of the SuperCam Mast Unit instrument, the microphone is directly exposed to the Martian environment. As a consequence, six microphone assemblies have undergone a package qualification and verification process (PQV) that consist of 1400 thermal summer cycles (+40 to -105 °C) and 600 winter cycles (+15 to -130 °C). No major potting lift off was observed that would endanger the cleanliness or the sealing of the RWEB, or the integrity of the microphone itself. No degradation of the acoustic performance was observed during the whole campaign. The PQV was performed at CNES in a thermal chamber supplied with liquid nitrogen.

A sub-lot of five microphone assembly parts eligible for flight was tested for a cryogenic temperature qualification at ISAE-SUPAERO in a dedicated thermal vacuum chamber operating with a liquid nitrogen thermal exchanger. The parts were mounted on a copper mechanical interface, as shown in Fig. 27, and the temperature of each assembly was monitored thanks to its internal PT100 sensor. Four cycles were performed from +60 °C to -135 °C: two of them under cruise pressure conditions (10^{-5} mbar), the microphone being off, and two under Martian conditions (5 to 10 mbar) with a functional test on the dwells. The performances of each assembly have been compared to their pre-qualification characteristics with the acoustic test bench. No measurable differences were observed and the five microphone assemblies were, therefore, declared qualified for the mission thermal environment. The flight model and its spare were picked from this sub-lot.

Fig. 26 Microphone test flow summary. Two tracks were used: (left) a track for the qualification, and (right) a track for the complete package qualification and verification (PQV)

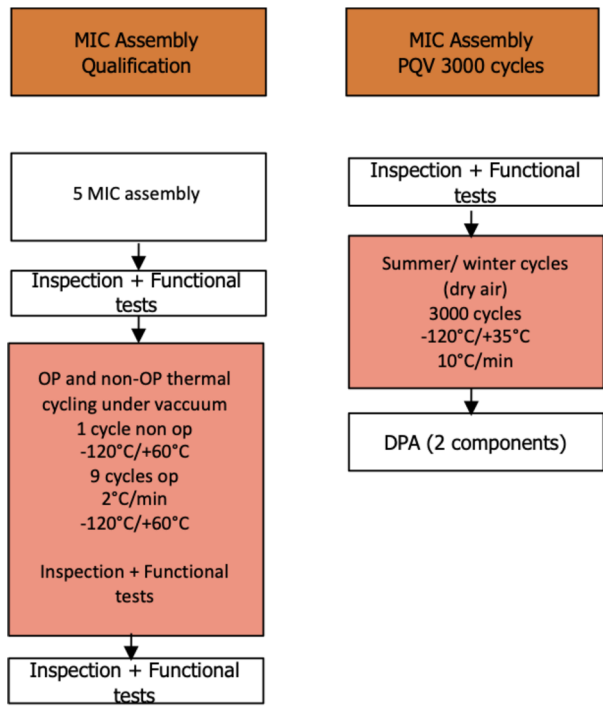
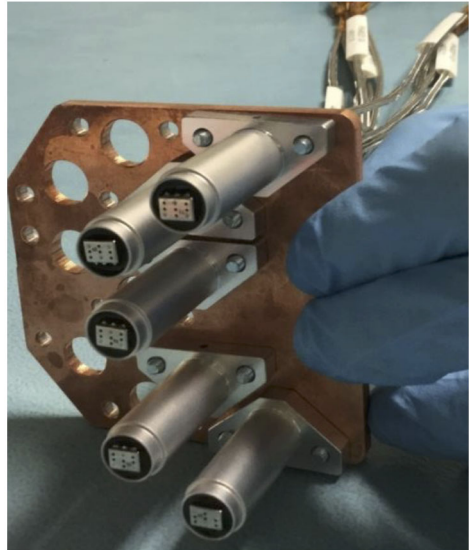


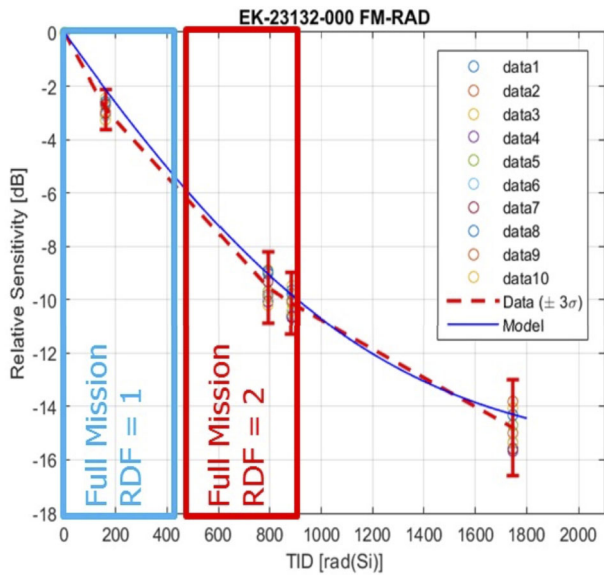
Fig. 27 Picture of the 5 microphone assemblies mounted on the copper interface for cryogenic temperature qualification



5.2 Radiation Susceptibility

Screening and lot qualification were performed on 100 microphone parts. The qualification path included detailed component analyses, and radiation sensitivity evaluation, with increasing ionizing doses up to 1750 rad (Si).

Fig. 28 Relative sensitivity of the EK-23132 as a function of the total ionizing dose (TID) measured during the radiation susceptibility assessment campaign). The blue curve is the model of microphone sensitivity degradation, and the red curve the best fit of the set of experimental measurements (data 1 to 10)



A group of ten microphone parts was dedicated to the total ionizing dose degradation analysis. As the microphone membrane is made of a permanently charged polymer, it is sensitive to radiation degradation. This degradation is probably due to the release of charge carriers in the medium during energy deposition. The radiation test was performed with five components powered to their nominal mission voltage of 3.3 V and five other components not powered. Components were irradiated with gamma rays from a Co60 source, and removed for testing at different Total Ionizing Dose (TID) values. The sensitivity comparison was established by comparing the components response to an acoustic sweep signal with respect to the response of a component not exposed to radiation. The excitation signal was generated by a speaker inside the test bench. The results of the relative sensitivity decay as a function of TID is presented in Fig. 28. The full mission equivalent dose is presented for Radiation Design Factors (RDF) of 1 and 2. According to the M2020 rover team analyses, the microphone will undergo most of the dose exposure during the cruise to Mars, to reach a worst-case end-of-life loss of sensitivity of -10 dB after 2 years, which is still compliant with the performance requirements.

5.3 Microphone Directivity

In order to assess the directivity of the microphone measurement, we have also studied the influence of the Mast Unit orientation on the microphone recording (Chide 2020). This measurement has been done in an anechoic chamber at ISAE-SUPAERO/DEOS Department (see picture of the setup in Fig. 29).

The directional sensitivity of the microphone has been studied, as well as the impact of the Mast Unit on this sensitivity. Full results are described in Chide (2020) and are summarized in Fig. 30.

On the left of Fig. 30, we see that the microphone is omnidirectional as specified in the microphone part data sheet. However, when the microphone is accommodated on the SuperCam Mast Unit, there is directionality obviously linked to the presence of the Mast Unit. In the forwards-facing direction, the sensitivity remains good.

Fig. 29 Picture of the SuperCam Mast Unit mock-up including the microphone in the anechoic chamber at ISAE-SUPAERO/DEOS Department

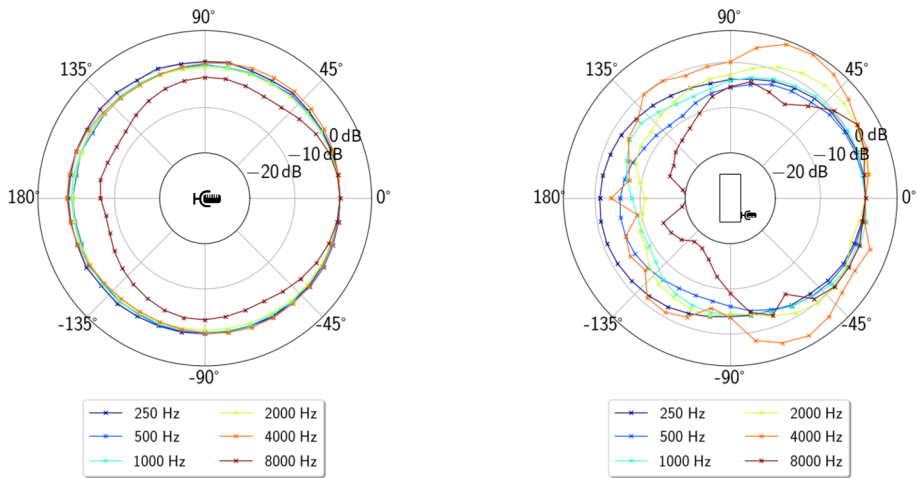
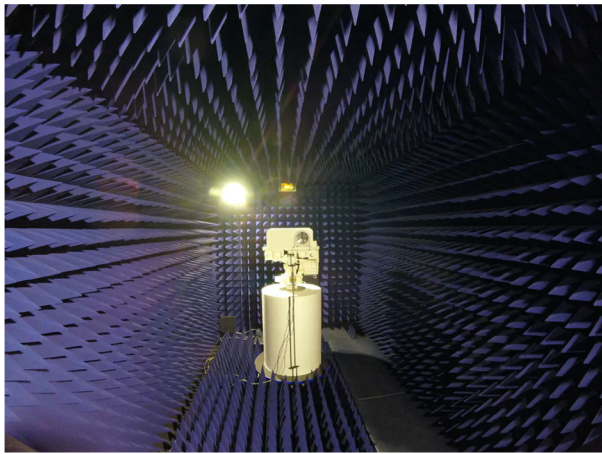


Fig. 30 Microphone Directivity. Left: Directivity of the microphone only. Right: Directivity of the microphone implemented on the Mast Unit. Figures from Chide (2020)

5.4 End-to-end Noise Characterization and Signal Validation

Since the clean rooms and thermal vacuum chamber are generally noisy environments in terms of acoustic measurement, the opportunities to get the complete system noise characterization are rare or non-existent. However, it happened to be possible in the LESIA facilities during the infrared spectrometer (IRS) qualification and characterization campaign. Figure 31 presents the comparison of the noise measurements of the microphone, integrated to the SuperCam Mast Unit, with the theoretical models for all gains, under 6 mbar of nitrogen. The model is a combination of the FEE noise model, the ADC quantification error model, and a microphone component noise model fitted with the data acquired during in the previous Martian wind tunnel test campaigns. The close match between the model and data validates the complete noise model of the SuperCam Microphone, which is used to distinguish the intrinsic instrument noise from the real acoustic signals in the scientific analyzes.

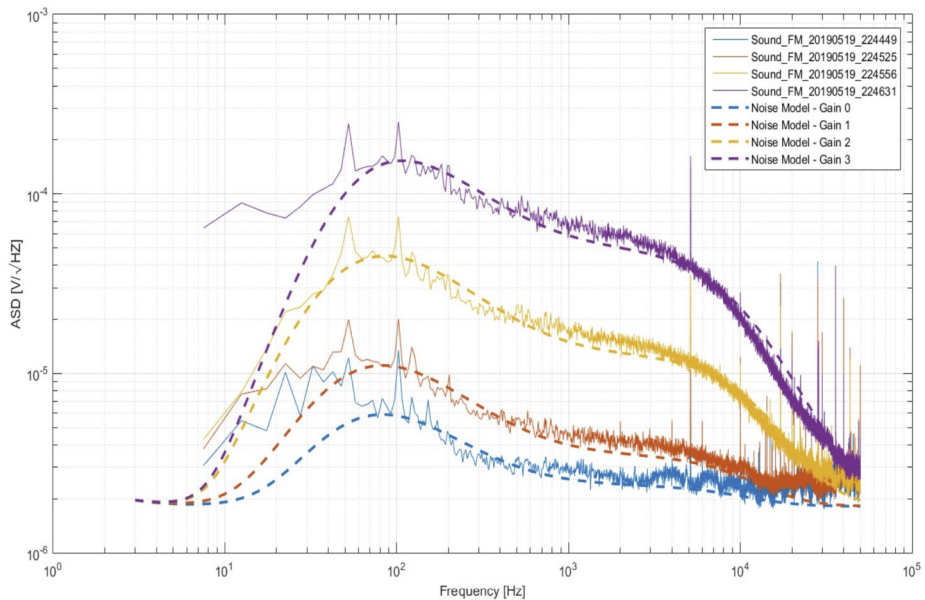


Fig. 31 Comparison between the noise amplitude spectral density models (noisy curve) and measurements (dashed line) of the microphone and its electronics integrated on to the SuperCam Mast Unit for all gains. The recording was performed at LESIA, in a thermal vacuum chamber under 6 mBar of N₂

During the system thermal test of the rover Perseverance at JPL, a raster of the LIBS laser shooting at the titanium calibration target was recorded with the microphone under a pressure of 6 mbar at -55 °C. The microphone was set to its minimum gain and successfully acquired 30 laser acoustic waveforms. A zoom on one waveform can be seen in Fig. 32. The maximum amplitude is 0.7 V and the root mean square noise level is 10 mV, leading to an operation re-calibration Signal-to-noise ratio (SNR) close to 60 dB, which is large when compared to the expected signal levels from the distant Martian rocks (20 to 30 dB). This calibration recording, and those acquired on Mars, are used to optimize the data processing pipeline currently under development, aiming at automatically extracting the relevant information from the waveforms, while removing most of the noise components.

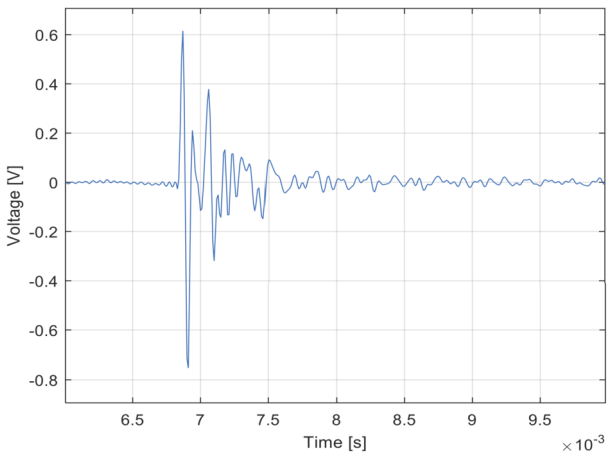
This acquisition, just before the rover integration into the interplanetary probe, was the last signal acquired by the microphone on Earth, and it validates the complete system chain of the flight model, from the calibration target up to the rover and the ground system.

5.5 Mars-like Environment Performance Validation

In order to validate the end-to-end performance of the instrument, full tests were performed using the Aarhus Wind Tunnel Simulator II (Holstein-Rathlou et al. 2014) in Denmark in July 2017. See Fig. 33 for a description of the test setup. The full details of these tests are reported in Murdoch et al. (2019). The AWTSII facility is a climatic chamber with a wind tunnel; it has a cylindrical shape, with a 2.1 m inner diameter, and a 10 m length. The tests were performed at 6 mbar of 100% CO₂. A suite of environmental sensors (temperature, pressure, humidity), in addition to an in-situ webcam, were used to monitor the environment.

These tests were the final validation that the acoustic signal of a laser LIBS blast could be recorded by the SuperCam Microphone in a Martian atmosphere environment at a 4 m

Fig. 32 Zoom on an acoustic waveform microphone measurement of a LIBS shot on a titanium calibration target at gain 0. The recording was performed during the system thermal test (STT) of the Perseverance rover at Jet Propulsion Laboratory (JPL), under 6 mbar of N₂ at -55 °C



distance (this was the science requirement). A peak SNR of 21 dB was measured, largely above the instrument SNR requirement of 10 dB. Thanks to this experiment, we also learned two important points:

1. These experiments demonstrated that wind signal would be recorded, as it adds a high amplitude, low frequency, component to the acoustic signal. However, this wind signal can be removed with relatively simple filtering, enabling LIBS recording even in windy conditions.
2. As a result of this, the microphone recording provides a good proxy for the wind speed, as already discussed in Sect. 2.4.2.

6 SuperCam Microphone Operations

6.1 Operational Limitations

They are several limitations in the use of the microphone that were taken into account during the ATLO process.

1. The maximum temperature that the microphone membrane can sustain without permanent degradation is +63 °C. Beyond that limit, the membrane polymer changes state, and the permanent electric dipole starts decreasing.
2. It has been observed that under pressure lower than 1 mBar, the microphone membrane resonance is not sufficiently damped, which creates a very strong oscillation when interacting with the electrostatic feedback force. Even though no degradation of the performances has been detected after vacuum testing, it is not recommended to power on the microphone under those conditions.
3. Membrane protection: in order to optimize its sensitivity, no filter has been implemented to protect the membrane from external objects.

6.2 In Situ Calibration

In order to have the best possible performance on Mars, we have to perform in-situ calibrations, that will enable to estimate the microphone best gain tuning, the microphone sensitivity to wind as well as the graceful performance degradation along the mission.

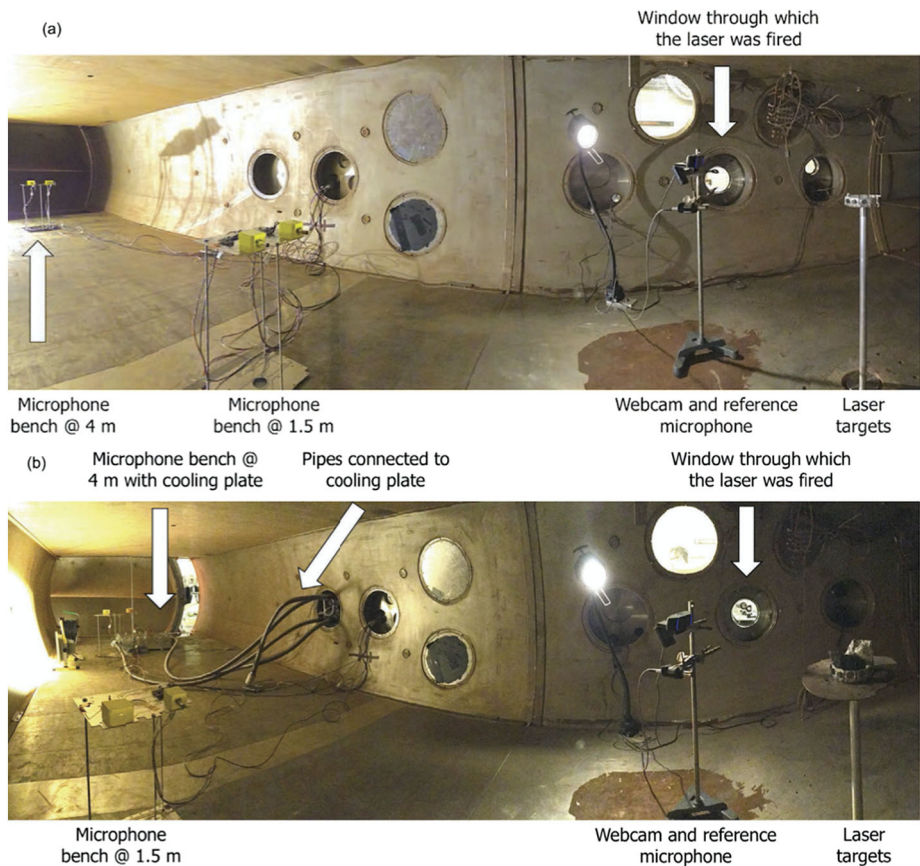


Fig. 33 Panoramic photos of the two test configurations at Aarhus. Above: First test configuration. Below: Second (low-temperature) test configuration. From Murdoch et al. (2019)

6.2.1 Sensor Cross Validation

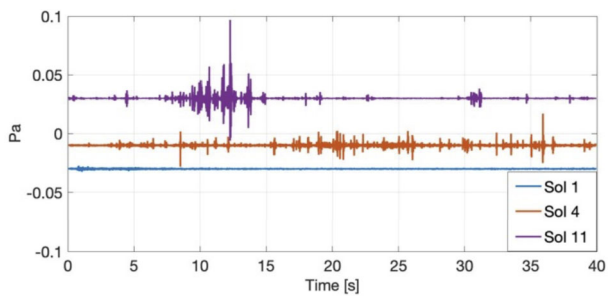
In order to evaluate the microphone sensitivity to the wind, we propose to record a stand-alone continuous sequence with SuperCam mast rotation in azimuth together with MEDA (1 recording for each Mast Unit position).

1. 15° or 30° steps in azimuth, elevation at 0°, 24 or 12 measurements in total
2. One 30 long microphone recording (25 kHz) per step in azimuth
3. Microphone measurements in parallel with MEDA to obtain wind speed and orientation
4. Ideally this sequence should not be executed for a wind coming from the rear of the rover, subject to too much interaction with the body of the rover and the RTG.

6.2.2 Regular Calibration

Each time a target calibration is performed, LIBS continuous recording shall be executed during shots on calibration targets. 4 sequences (gains 0, 1, 2, 3) shall be executed, 100 kHz. In particular, LIBS+MIC shall be executed each time the SuperCam Calibration Target

Fig. 34 First Microphone passive recordings during sol 1, Sol 4 and 11



(SCCT) Titanium is targeted: it will be used as the in-situ reference sound as acoustic LIBS signal on titanium is loud and because the ablation rate on titanium is small. Therefore, the acoustic signal should remain relatively constant with the number of shots. This should allow the graceful performance degradation of the microphone to be characterized as a function of time. MIC ONLY recording shall be executed routinely in parallel with MEDA (one pointing only) to calibrate the microphone RMS pressure level with regard to wind speed. The LIBS+MIC measurements will also have to take into account the variation of the LIBS signal as a function of the external pressure and other atmospheric variables (which vary between seasons).

7 SuperCam Microphone Early Results

7.1 First Sols Recordings

The Mars microphone was operated several times during the first days of the Mars 2020 rover on Mars (Sol 1, 4 and 11), as depicted in Fig. 34. During the first recording, the Mast Unit was stowed and, therefore, the sound recorded was muffled. However, a distinct aeolian signature can be heard. During these first sols, the microphone was operated in a passive (MIC only) mode, recording the acoustic environment.

On sol 12, the microphone recorded the sound of the LIBS signal on Mars for the first time (see Fig. 35), validating the concept of operation. The various gains of the microphone FEE also proved to be adapted to the Martian environment.

7.2 Use of the Microphone During the First Year of Perseverance Operations

The microphone has been used regularly during the first 450 sols of Mars operation of the Mars 2020 rover. Several hours of Mars sound recording are now available. Figure 34 makes a summary of the recording types up to sol 450 as a function of the local mean solar time Local Mean Solar Time (LMST) of recording. The diversity of timing actually represents the variety of goals, with passive recordings mostly dedicated to atmospheric study spread over all local times, and LIBS recording mostly at noon.

A summary of most significant scientific results from the first year of measurement can be found in Maurice et al. (2022).

8 Conclusions and Discussion

The SuperCam Microphone has been the first microphone to record sounds from the surface of Mars. It has been able to record audio signals from 20 Hz to 10 kHz with a sensitivity

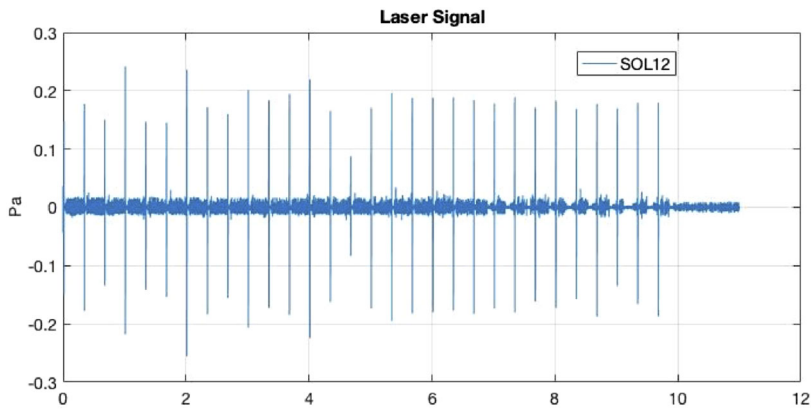


Fig. 35 First Microphone LIBS recordings during sol 12

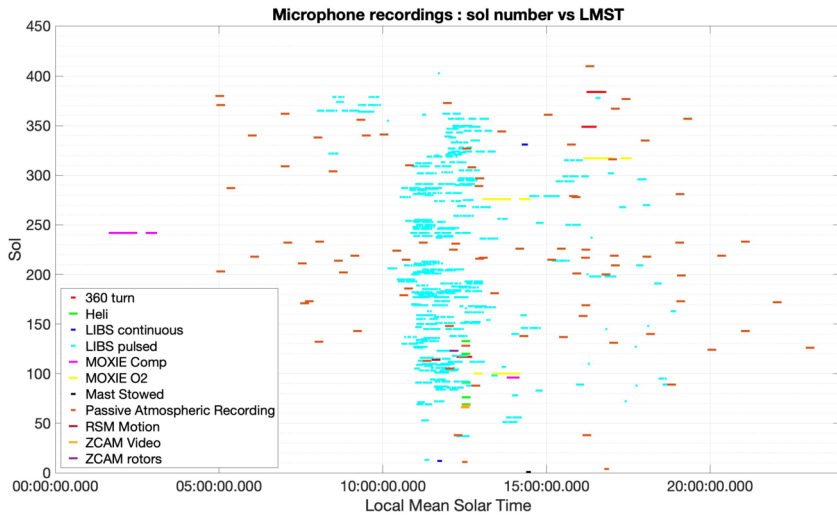


Fig. 36 Summary of all microphone recordings up to sol 450. X-axis is LMST, and Y-axis figures the sol

sufficient to monitor a LIBS shock wave at distances of up to 4 m. The acoustic environment of Mars was not understood before the Perseverance rover's arrival. A year of microphone operation has allowed us to understand that, most of the time, Mars is very quiet. In addition, LIBS and helicopter recordings have helped us to provide additional constraints on carbon dioxide acoustic attenuation models. Even if the SuperCam Microphone primary goal is characterizing the rocks shot by SuperCam, the microphone has so far opened a new window of atmospheric measurement on the Mars surface, providing high frequency insights on the wind and turbulence measurements.

Acknowledgements We gratefully acknowledge funding from the French space agency (CNES), from ISAE-SUPAERO, and from Région Occitanie. The authors would also like to thank Ralph Lorenz for his useful insights on the historical part.

Declarations

Competing Interests The authors declare no competing interests.

References

- Balme M, Greeley R (2006) Dust devils on Earth and Mars. *Rev Geophys* 44:RG3003. <https://doi.org/10.1029/2005RG000188>
- Banerdt WB, Smrekar SE, Banfield D, Giardini D, Golombek M, Johnson CL, Lognonné P, Spiga A, Spohn T, Perrin C et al (2020) Initial results from the insight mission on Mars. *Nat Geosci* 13(3):183–189. <https://doi.org/10.1038/s41561-020-0544-y>
- Bass HE, Chambers JP (2001) Absorption of sound in the Martian atmosphere. *J Acoust Soc Am* 109(6):3069–3071. <https://doi.org/10.1121/1.1365424>
- Bell JF, Maki JN, Mehall GL, Ravine MA, Caplinger MA, Bailey ZJ, Brylow S, Schaffner JA, Kinch KM, Madsen MB et al (2021) The Mars 2020 Perseverance rover mast camera zoom (Mastcam-Z) multi-spectral, stereoscopic imaging investigation. *Space Sci Rev* 217:24. <https://doi.org/10.1007/s11214-020-00755-x>
- Chaleard C, Mauchien P, Andre N, Uebbing J, Lacour JL, Geertsen C (1997) Correction of matrix effects in quantitative elemental analysis with laser ablation optical emission spectrometry. *J Anal At Spectrom* 12(2):183–188
- Chatain A, Spiga A, Banfield D, Forget F, Murdoch N (2021) Seasonal variability of the daytime and nighttime atmospheric turbulence experienced by InSight on Mars. *Geophys Res Lett* 48:e2021GL095453. <https://doi.org/10.1029/2021GL095453>
- Chide B (2020) Le premier microphone sur Mars: contribution à la spectroscopie de plasma induit par laser et à la science atmosphérique. PhD thesis, Toulouse, ISAE. <http://www.theses.fr/2020ESAE0041>
- Chide B, Maurice S, Murdoch N, Lasue J, Bousquet B, Jacob X, Cousin A, Forni O, Gasnault O, Meslin P-Y, Fronton J-F, Bassas-Portús M, Cadu A, Sournac A, Mimoun D, Wiens RC (2019) Listening to laser sparks: a link between Laser-Induced Breakdown Spectroscopy, acoustic measurements and crater morphology. *Spectrochim Acta* 153:50–60. <https://doi.org/10.1016/j.sab.2019.01.008>
- Chide B, Murdoch N, Bury Y, Maurice S, Jacob X, Merrison JP, Iversen JJ, Meslin P-Y, Bassas-Portús M, Cadu A, Sournac A, Dubois B, Lorenz RD, Mimoun D, Wiens RC (2021) Experimental wind characterization with the SuperCam microphone under a simulated Martian atmosphere. *Icarus* 354:114060. <https://doi.org/10.1016/j.icarus.2020.114060>
- Dehant V, Lognonné P, Sotin C (2004) Network science, NetLander: a European mission to study the planet Mars. *Planet Space Sci* 52(11):977–985
- Delory GT, Luhmann J, Friedman L, Betts B (2007) Development of the first audio microphone for use on the surface of Mars. *J Acoust Soc Am* 121(5):3116
- Esposito F, Debei S, Bettanini C, Molfese C, Arruego Rodríguez I, Colombatti G, Harri A-M, Montmessin F, Wilson C, Aboudan A et al (2013) DREAMS for the ExoMars 2016 mission: a suite of sensors for the characterization of Martian environment. In: European planetary science congress, pp EPSC2013-815
- Farley KA, Williford KH, Stack KM, Bhartia R, Chen A, de la Torre M, Hand K, Goreva Y, Herd CDK, Hueso R et al (2020) Mars 2020 mission overview. *Space Sci Rev* 216:142. <https://doi.org/10.1007/s11214-020-00762-y>
- Ferri F, Smith PH, Lemmon M, Rennó NO (2003) Dust devils as observed by Mars Pathfinder. *J Geophys Res, Planets* 108(E12):5133. <https://doi.org/10.1029/2000JE001421>
- Grad L, Možina J (1993) Acoustic in situ monitoring of excimer laser ablation of different ceramics. *Appl Surf Sci* 69(1):370–375. [https://doi.org/10.1016/0169-4332\(93\)90536-K](https://doi.org/10.1016/0169-4332(93)90536-K)
- Hecht M, Hoffman J, Rapp D, McClean J, SooHoo J, Schaefer R, Aboobaker A, Mellstrom J, Hartvigsen J, Meyen F et al (2021) Mars Oxygen ISRU Experiment (MOXIE). *Space Sci Rev* 217:9. <https://doi.org/10.1007/s11214-020-00782-8>
- Holstein-Rathlou C, Merrison J, Iversen JJ, Jakobsen AB, Nicolajsen R, Nørnberg P, Rasmussen K, Merlone A, Lopardo G, Hudson T et al (2014) An environmental wind tunnel facility for testing meteorological sensor systems. *J Atmos Ocean Technol* 31(2):447–457
- Ksanfomaliti LV, Goroshkova NV, Naraeva MK, Suvorov AP, Khondryev VK, Yabrova LV (1982) Acoustic measurements of the wind velocity at the Venera-13 and Venera-14 landing sites. *Sov Astron Lett* 8:227–229
- Ksanfomaliti LV, Goroshkova NV, Khondryev VK (1983) Wind velocity on the Venus surface from acoustic measurements. *Kosm Issled* 21:218–224

- Lanza NL, Chide B, Clegg SM, Dauson E, Forni O, Larmat C, Ollila AM, Reyes-Newell A, Ten Cate J, Wiens RC et al (2020) Listening for rock coatings on Mars: using acoustic signals from laser-induced breakdown spectroscopy to identify surface coatings and layers. In: Lunar and planetary science conference, vol 51, p 2807
- Lanza N, Chide B, Mimoun D, Alvarez C, Angel S, Bernardi P, Beyssac O, Bousquet B, Cadu A, Clave E et al. (2021) Expected first results from the SuperCam microphone onboard the NASA Perseverance rover. Technical report, Copernicus Meetings
- Leighton TG, White PR (2004) The sound of Titan: a role for acoustics in space exploration. *Acoust Bull* 29(4):16–23
- Lorenz RD, Christie D (2015) Dust devil signatures in infrasound records of the International Monitoring System. *Geophys Res Lett* 42(6):2009–2014. <https://doi.org/10.1002/2015GL063237>
- Lorenz RD, Merrison J, Iversen JJ (2017) Wind noise and sound propagation experiments in the Aarhus Mars atmosphere simulation chamber. In: Sixth international workshop on the Mars atmosphere: modelling and observations, p 4405
- Maki JN, Gruel D, McKinney C, Ravine MA, Morales M, Lee D, Willson R, Copley-Woods D, Valvo M, Goodsall T et al (2020) The Mars 2020 engineering cameras and microphone on the Perseverance rover: a next-generation imaging system for Mars exploration. *Space Sci Rev* 216:137. <https://doi.org/10.1007/s11214-020-00765-9>
- Malin MC, Caplinger MA, Edgett KS, Ghaemi FT, Ravine MA, Schaffner JA, Maki JN, Willson RG, Bell JF, Cameron JF et al (2009) The Mars Science Laboratory (MSL) Mars Descent Imager (MARDI) flight instrument. In: 40th annual lunar and planetary science conference, p 1199
- Mangold N, Gupta S, Gasnault O, Dromart G, Tarnas SJ, Sholes SF, Horgan B, Quantin-Nataf C, Brown AJ, Le Mouélic S et al (2021) Perseverance rover reveals an ancient delta-lake system and flood deposits at Jezero crater, Mars. *Science* 374(6568):711–717
- Martire L, Garcia RF, Rolland L, Spiga A, Henri Lognonné P, Banfield D, Banerdt WB, Martin R (2020) Martian infrasound: numerical modeling and analysis of InSight's data. *J Geophys Res, Planets* 125(6):e2020JE006376
- Maurice S, Wiens RC, Saccoccio M, Barraclough B, Gasnault O, Forni O, Mangold N, Baratoux D, Bender S, Berger G et al (2012) The ChemCam instrument suite on the Mars Science Laboratory (MSL) rover: science objectives and mast unit description. *Space Sci Rev* 170(1–4):95–166. <https://doi.org/10.1007/s11214-012-9912-2>
- Maurice S, Wiens RC, Bernardi P, Cais P, Robinson S, Nelson T, Gasnault O, Reess JM, Deleuze M, Rull F, Manrique JA, Abbaki S, Anderson RB, André Y, Angel SM, Arana G, Battault T, Beck P, Benzerara K, Bernard S, Berthias JP, Beyssac O, Bonafous M, Bousquet B, Boutillier M, Cadu A, Castro K, Chapron F, Chide B, Clark K, Clavé E, Clegg S, Cloutis E, Collin C, Cordoba EC, Cousin A, Dameury JC, D'Anna W, Daydou Y, Debuss A, Deflores L, Dehouck E, Delapp D, De Los Santos G, Donny C, Doressoundiram A, Dromart G, Dubois B, Dufour A, Dupieux M, Egan M, Ervin J, Fabre C, Fau A, Fischer W, Forni O, Fouchet T, Frydenvang J, Gauffre S, Gauthier M, Gharakanian V, Gilard O, Gontijo I, Gonzalez R, Granena D, Groszinger J, Hassen-Khodja R, Heim M, Hello Y, Hervet G, Humeau O, Jacob X, Jacquiod S, Johnson JR, Kouach D, Lacombe G, Lanza N, Lapauw L, Laserna J, Lasue J, Le Deit L, Le Mouélic S, Le Comte E, Lee QM, Legett C, Leveille R, Lewin E, Leyrat C, Lopez-Reyes G, Lorenz R, Lucero B, Madariaga JM, Madsen S, Madsen M, Mangold N, Manni F, Mariscal JF, Martinez-Frias J, Mathieu K, Mathon R, McCabe KP, McConnochie T, McLennan SM, Mekki J, Melikechi N, Meslin PY, Micheau Y, Michel Y, Michel JM, Mimoun D, Misra A, Montagnac G, Montaron C, Montmessin F, Moros J, Mousset V, Morizet Y, Murdoch N, Newell RT, Newsom H, Nguyen Tuong N, Ollila AM, Orttner G, Oudda L, Pares L, Parisot J, Parot Y, Pérez R, Pheav D, Picot L, Pilleri P, Pilorget C, Pinet P, Pont G, Poulet F, Quantin-Nataf C, Quartier B, Rambaud D, Rapin W, Romano P, Roucaurol L, Royer C, Ruellan M, Sandoval BF, Sautter V, Schoppers MJ, Schröder S, Seran HC, Sharma SK, Sobron P, Sodki M, Sournac A, Sridhar V, Standaarovsky D, Storms S, Striebig N, Tatat M, Toplis M, Torre-Fdez I, Toulemon N, Velasco C, Veneranda M, Venhaus D, Virmontois C, Viso M, Willis P, Wong KW (2021) The SuperCam instrument suite on the Mars 2020 rover: science objectives and Mast-Unit description. *Space Sci Rev* 217(3):47. <https://doi.org/10.1007/s11214-021-00807-w>
- Maurice S, Chide B, Murdoch N, Lorenz RD, Mimoun D, Wiens RC, Stott A, Jacob X, Bertrand T, Montmessin F et al (2022) In situ recording of Mars soundscape. *Nature* 605(7911):653–658. <https://doi.org/10.1038/s41586-022-04679-0>
- Mimoun D, Murdoch N, Lognonné P, Hurst K, Pike WT, Hurley J, Nébut T, Banerdt WB (SEIS Team) (2017) The noise model of the SEIS seismometer of the InSight mission to Mars. *Space Sci Rev*. <https://doi.org/10.1007/s11214-017-0409-x>
- Morgan S, Raspet R (1992) Investigation of the mechanisms of low-frequency wind noise generation outdoors. *J Acoust Soc Am* 92(2):1180–1183

- Muirhead BK, Nicholas AK, Umland J, Sutherland O, Vijendran S (2020) Mars sample return campaign concept status. *Acta Astronaut* 176:131–138
- Murdoch N, Chide B, Lasue J, Cadu A, Sournac A, Bassas-Portús M, Jacob X, Merrison J, Iversen JJ, Moretto C, Velasco C, Parès L, Hynes A, Godiver V, Lorenz RD, Cais P, Bernadi P, Maurice S, Wiens RC, Mimoun D (2019) Laser-induced breakdown spectroscopy acoustic testing of the Mars 2020 microphone. *Planet Space Sci* 165:260–271. <https://doi.org/10.1016/j.pss.2018.09.009>
- Murdoch N, Lorenz R, Chide B, Cadu A, Stott A, Maurice S, Wiens RC, Mimoun D (2021a) Predicting signatures of dust devils recorded by the SuperCam microphone. In: Lunar and planetary science conference, vol 2548, p 1658
- Murdoch DM, Stott AE, Chide B, Lorenz R, Maurice S, de la Torre Juárez M, Newman C, Wolff M, Wiens RC (2021b) The Perseverance acoustics, and atmospheric working groups. Atmospheric science with the SuperCam microphone on the Perseverance rover. In: Europlanet science congress, vol 2548, pp EPSC2021-516. <https://doi.org/10.5194/epsc2021-516>
- Murphy J, Steakley K, Balme M, Deprez G, Esposito F, Kahanpää H, Lemmon M, Lorenz R, Murdoch N, Neakrase L et al (2016) Field measurements of terrestrial and Martian dust devils. *Space Sci Rev* 203(1):39–87. <https://doi.org/10.1007/s11214-016-0283-y>
- Perrin C, Rodriguez S, Jacob A, Lucas A, Spiga A, Murdoch N, Lorenz R, Daubar IJ, Pan L, Kawamura T et al (2020) Monitoring of dust devil tracks around the InSight landing site, Mars, and comparison with in situ atmospheric data. *Geophys Res Lett* 47(10):e2020GL087234. <https://doi.org/10.1029/2020GL087234>
- Qin Q, Attenborough K (2004) Characteristics and application of laser-generated acoustic shock waves in air. *Appl Acoust* 65(4):325–340. <https://doi.org/10.1016/j.apacoust.2003.11.003>
- Rehse S (2021) What is LIBS? University of Windsor <https://www.uwindsor.ca/people/rehse/299/libs>, November 2021
- Rodriguez-Manfredi JA, de la Torre Juárez M, Alonso A, Apéstigue V, Arruego I, Atienza T, Banfield D, Boland J, Carrera MA, Castañer L et al (2021) The Mars Environmental Dynamics Analyzer, MEDA. A suite of environmental sensors for the Mars 2020 mission. *Space Sci Rev* 217:48. <https://doi.org/10.1007/s11214-021-00816-9>
- Smith PH (2004) The Phoenix mission to Mars. In: 2004 IEEE aerospace conference proceedings (IEEE cat. no. 04TH8720), vol 1. IEEE Press, New York
- Sparrow VW (1999) Acoustics on the planet Mars: a preview. *J Acoust Soc Am* 106(4):2264
- Spiga A, Teanby NA, Forget F, Lucas A, Banfield D et al (2018) Atmospheric Science with InSight. *Space Sci Rev* 214:109. <https://doi.org/10.1007/s11214-018-0543-0>
- Temel O, Senel CB, Spiga A, Murdoch N, Banfield D, Karatekin O (2022) Spectral analysis of the Martian atmospheric turbulence: InSight observations. *Geophys Res Lett* 49(15):e2022GL099388. <https://doi.org/10.1029/2022GL099388>
- Tillman JE, Landberg L, Larsen SE (1994) The boundary layer of Mars: fluxes, stability, turbulent spectra, and growth of the mixed layer. *J Atmos Sci* 51(12):1709–1727
- Ullán A, Zorzano M-P, Martín-Torres FJ, Valentín-Serrano P, Kahanpää H, Harri A-M, Gómez-Elvira J, Navarro S (2017) Analysis of wind-induced dynamic pressure fluctuations during one and a half Martian years at Gale Crater. *Icarus* 288:78–87. <https://doi.org/10.1016/j.icarus.2017.01.020>
- Wiens RC, Maurice S, Robinson SH, Nelson AE, Cais P, Bernardi P, Newell RT, Clegg S, Sharma SK, Storms S, Deming J, Beckman D, Ollila AM, Gasnault O, Anderson RB, André Y, Angel SM, Arana G, Auden E, Beck P, Becker J, Benzerara K, Bernard S, Beyssac O, Borges L, Bousquet B, Boyd K, Caffrey M, Carlson J, Castro K, Celis Baptiste Chide J, Clark K, Cloutis E, Cordoba EC, Cousin A, Dale M, Deflores L, Delapp D, Deleuze M, Dirmyer M, Donny C, Dromart G, George Duran M, Egan M, Ervin J, Fabre C, Fau A, Fischer W, Forni O, Fouchet T, Fresquez R, Frydenvang J, Gasway D, Gontijo I, Grotzinger J, Jacob X, Jacquino S, Johnson JR, Klisiewicz RA, Lake J, Lanza N, Laserna J, Lasue J, Le Mouélic S, Leggett C, Leveillé R, Lewin E, Lopez-Reyes G, Lorenz R, Lorigny E, Love SP, Lucero B, Madariaga JM, Madsen M, Madsen S, Mangold N, Manrique JA, Martinez JP, Martinez-Frias J, McCabe KP, McConnochie TH, McGlown JM, McLennan SM, Melikechi N, Meslin P-Y, Michel JM, Mimoun D, Misra A, Montagnac G, Montmessin F, Mousset V, Murdoch N, Newsom H, Ott LA, Ousnamer ZR, Pares L, Parot Y, Pawluczky R, Glen Peterson C, Pilleri P, Pinet P, Pont G, Poulet F, Provost C, Quertier B, Quinn H, Rapin W, Reess J-M, Regan AH, Reyes-Newell AL, Romano PJ, Royer C, Rull F, Sandoval B, Sarrao JH, Sautter V, Schoppers MJ, Schröder S, Seitz D, Shepherd T, Sobron P, Dubois B, Sridhar V, Toplis MJ, Torre-Fdez I, Trettel IA, Underwood M, Valdez A, Valdez J, Venhaus D, Willis P (2021) The SuperCam instrument suite on the NASA Mars 2020 rover: body unit and combined system tests. *Space Sci Rev* 217(1):4. <https://doi.org/10.1007/s11214-020-00777-5>
- Williams J-P (2001) Acoustic environment of the Martian surface. *J Geophys Res* 106:5033–5042. <https://doi.org/10.1029/1999JE001174>

Authors and Affiliations

David Mimoun¹  · Alexandre Cadu¹ · Naomi Murdoch¹ · Baptiste Chide² · Anthony Sournac¹ · Yann Parot² · Pernelle Bernardi³ · P. Pilleri² · Alexander Stott¹ · Martin Gillier¹ · Vishnu Sridhar⁴ · Sylvestre Maurice² · Roger Wiens⁵ · the SuperCam team

✉ D. Mimoun
david.mimoun@isae.fr

A. Cadu
alexandre.cadu@isae.fr

N. Murdoch
naomi.murdoch@isae.fr

B. Chide
baptiste.chide@irap.omp.fr

A. Sournac
Anthony.Sournac@isae.fr

Y. Parot
yann.parot@irap.omp.fr

P. Bernardi
pernelle.bernardi@obspm.fr

P. Pilleri
paolo.pilleri@irap.omp.fr

A. Stott
Alexander.Stott@isae.fr

M. Gillier
Martin.Gillier@isae.fr

V. Sridhar
vishnu.sridhar@jpl.nasa.gov

S. Maurice
sylvestre.maurice@irap.omp.eu

R. Wiens
rwiens@lanl.gov

¹ Institut Supérieur de l'Aéronautique et de l'Espace (ISAE-SUPAERO), Université de Toulouse, 31055 Toulouse Cedex 4, France

² Institut de Recherche En Astrophysique et Planétologie, Toulouse, France

³ Laboratoire d'Etudes Spatiale et d'Instrumentation en Astrophysique (LESIA), Paris, France

⁴ Jet Propulsion Laboratory, 4800 Oak Grove Dr, Pasadena, CA 91109, USA

⁵ Los Alamos National Laboratories, Los Alamos, NM 87544, USA